

1 **Title:** How did that get there? Understanding sediment transport and accumulation
2 rates in agricultural landscapes using the ESTTraP agent-based model.

3

4 **Authors:** Kabora, T.K.^a (corresponding author), Stump, D.^b & Wainwright, J.^c

5 ^a Department of Archaeology, University of York, The King's Manor
6 York, YO1 7EP, UK

7 ^b Department of Archaeology, University of York, The King's Manor
8 York, YO1 7EP, UK

9 ^c Department of Geography, Durham University, Lower Mountjoy
10 South Road, Durham, DH1 3LE, UK

11

12 Corresponding author's email and present address: tkkabora@gmail.com

13

14 **Abstract**

15 The 15th-18th century CE site of Engaruka in Tanzania is often described as primarily
16 comprising drystone agricultural terraces, but it is now known that many of these
17 former farming plots are not terraces *per se*, but are instead sediment traps.

18 Stratigraphic excavations of these traps show that they were built by constructing low
19 drystone walls adjacent to either natural or artificial water courses in order to capture
20 fine alluvial sediments entrained within water flows. In the northern area of the site
21 sediments were accumulated to a depth of up to 700 mm, while in one area in the
22 south of the site over 2 m of deposits were accumulated over at least a 300 year
23 period. The presence of sediment traps on archaeological sites allows investigations
24 of the efficacy and sustainability of these structures over decadal to centennial
25 timescales, since stratigraphic excavations can define the process of construction,
26 and geoarchaeological analyses can explore changes within accumulated sediments
27 over time. Although a combination of stratigraphy and absolute dating can discern
28 the broad sequence and timing of sediment capture they cannot determine
29 sediment-accumulation rates, and these techniques are too time consuming to be
30 used to map the development of over 9 km² of sediment traps. The ESTTraP agent-
31 based model provides these data by simulating sediment accumulation under
32 different hydrological conditions. Four scenarios were simulated for a period of 100
33 years: constant water availability (SIM-01), seasonal variability (SIM-02), long-term
34 climate variability (SIM-03), and vegetation-cover impact (SIM-04). The model

35 results suggest that the fields can be constructed over a short period of time,
36 approximately 1 - 3 months per 6 × 6 m field, and that to construct a block of 90
37 fields covering 3,000 m² it would take between 8 to 13 years in periods of high water
38 availability, and up to 27 years during prolonged dry periods. The results define the
39 amount of time needed to construct individual fields, and suggest that farmers
40 constructed blocks of fields concurrently rather than sequentially expanding across
41 the landscape, and that the c. 10 km² area of sediment traps at Engaruka could have
42 been constructed by a number of households working independently. The ESTTraP
43 model presents an important resource in the assessment of sediment dynamics and
44 patterns of field development, is relevant to a range of archaeological sites
45 worldwide that include intentional or unintentional alluvial deposition, and has
46 applications for modern landscape management.

47

48 **Highlights**

49 Technique for assessing long-term sustainability of sediment traps

50 Long-term patterns of sediment accumulation

51 Water availability the main constraint on sediment accumulation rates

52 Modelling of sediment accumulation helps refine site chronology

53 Landscape modifications can be achieved through house-hold level interventions

54

55 **Keywords**

56 Sediment transport

57 Sediment traps

58 Agent-based model

59 Engaruka

60 Water-management system

61 Sediment accumulation rates

62

63 **1. Introduction**

64 The construction of artificial sediment traps to create agricultural fields is a
65 widespread practice (Mekonnen, et al., 2015), and is increasingly being recognised
66 on archaeological sites. These include long-abandoned sites like Petra in Jordan
67 (Beckers, et al., 2013) and extant farming systems in Ethiopia and Tunisia (Ferro-
68 Vázquez, et al., 2017, Hill and Woodland, 2003), while other studies recognise

69 ancient sediment traps as exploitable legacies from previous periods of agricultural
70 expansion or intensification (Giráldez, et al., 1988). Sediment traps can be built in a
71 variety of ways and can perform one or more of several functions, including
72 mitigating the impacts of soil erosion, stabilising sedimentation, increasing soil depth
73 and soil-water storage capacity, reducing runoff or the velocity of channelled water,
74 accumulating fine sediments for ease of tillage or root penetration, the incorporation
75 of mineral or organic material beneficial to plant growth within agricultural plots, or to
76 create flat areas for cultivation within valleys or at the base the slopes (Mekonnen, et
77 al., 2015, Abedini, et al., 2012, Ran, et al., 2008). At the current case-study site of
78 Engaruka in Tanzania, geochemical results suggest that the repeated accumulation
79 of sediments within traps also avoided the salinization of soils (Lang and Stump,
80 2017); a common problem with prolonged irrigation, particularly in the tropics. The
81 ability of archaeological research to identify these benefits, and to assess their
82 efficacy over decadal to millennial scales, means it is well placed to contribute to
83 assessments of agricultural sustainability (Fisher, 2019, Logan, et al., 2019) Since
84 the construction of sediment traps leads to increases in the quantity of accumulated
85 sediments over time, they provide an ideal case-study of how archaeological data-
86 sets can be used to quantify change, and thus contribute to assessments of the
87 costs and benefits of human-landscape modifications. In the current paper we
88 employ agent-based modelling to explore the physical and environmental factors that
89 influence the rates of sediment accumulation with sediment traps at Engaruka, and
90 discuss why the rates of change are significant to questions of site chronology,
91 resource use, agricultural management, social hierarchy and sustainability.

92

93 Within the archaeological literature sediment traps are sometimes classified as a
94 form of runoff agriculture or as a runoff-terrace system (e.g. Beckers, et al., 2013,
95 Evenari, et al., 1982), reflecting the fact that water-harvesting systems can
96 unintentionally accumulate the sediments entrained within water flows, most
97 obviously in the infilling of artificial reservoirs (Morrison, 2015). For some issues of
98 relevance to agricultural management and sustainability, intentionality may not
99 matter: the periodic addition of new sediments may have mitigated the effects of soil
100 salinization at Engaruka, for example, but it cannot be concluded from this that the
101 farmers who built these traps were aware of this effect. The question of intentional or
102 unintentional accumulation of sediments remains important, however: the removal of

103 sediments inadvertently accumulated within irrigation canals, fields or reservoirs can
104 be a time-consuming and labour intensive process (Sheridan, 2002) and may prompt
105 their abandonment (Morrison, 2015) . At Engaruka, in contrast, the layout, method of
106 construction, and physical extent of the area of sediment traps, strongly suggest that
107 the farmers who built the field system between the 15th and 18th centuries CE
108 intended to exploit available river flows while deliberately capturing the sediments
109 they carried, in the process creating c.9 km² of sediment traps up to 700 mm deep in
110 the northern end of the site (Stump, 2016, Stump, 2006) , and accumulating
111 sediments over 2 m deep towards the southern end of the field system (Lang and
112 Stump, 2017).

113

114 The Engaruka system is of particular interest as excavations show that sediment
115 trapping and accumulation was inherently tied to the construction and expansion of
116 the system of drystone-bound fields bounded by drystone walls (Stump, 2006).
117 Studies by Lang and Stump (2017) and Stump (2006) show that the drystone walls
118 of the sediment- trap fields were not self-supporting and instead were supported by
119 the accumulation of sediments behind the walls. This arrangement meant that wall
120 courses were raised as the sediments accumulated in the sediment trap fields with
121 farmers placing additional drystone wall courses over time that raised the height of
122 the walls as the sediment depths increased. In addition, excavations (Stump, 2006)
123 also showed that the sediment trap fields were built in a series of blocks with each
124 block surrounded by a set of canals that transported the water and sediments to
125 these fields (Fig. 2). Thus the rate of sediment accumulation influenced the
126 construction of the drystone fields and the expansion of the field system across the
127 landscape.

128

129 Although studies of archaeological stratigraphy can define the depth and extent of
130 sediment accumulation, and can demonstrate broadly the sequence of sediment-trap
131 construction, this approach provides little data on rates of sedimentation, and hence
132 the rate, pattern and manner of the system's development. The aim of this study is
133 thus to assess the effects of water- and sediment-transport dynamics on sediment
134 accumulation and field development at Engaruka. In this paper we use evidence
135 from archaeological excavations, field survey and aerial photographic data to create
136 a simulated version of the North Fields area at Engaruka, and employ agent-based

137 modelling (ABM) techniques to simulate different hydrological scenarios based on
138 data from modern irrigation at Engaruka and palaeoclimatic data from the region
139 (Ryner, et al., 2008, Verschuren, et al., 2000).

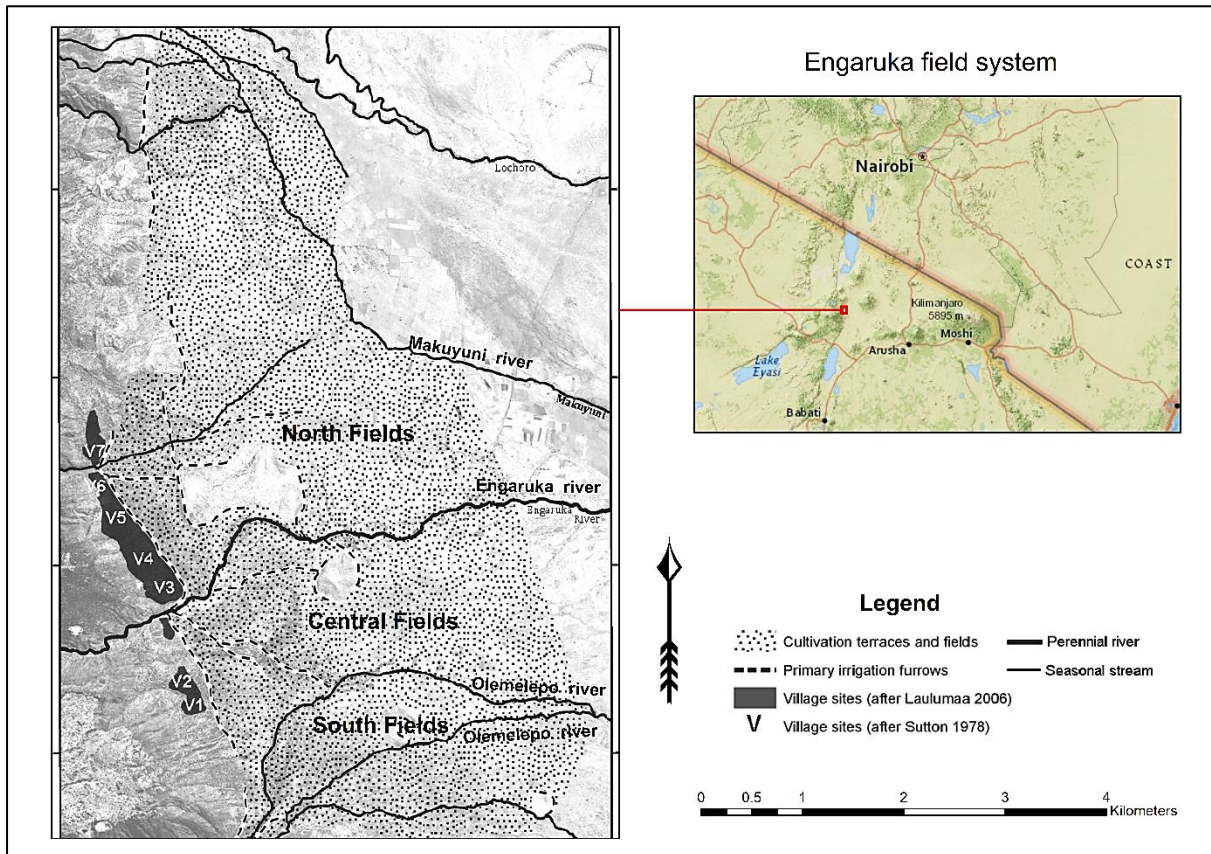
140

141 ABM represents just one technique that can be used to approach this problem, with
142 others including 'system dynamics' - a deterministic, top-down modelling approach
143 that provides an aggregate view of the system's processes (Ding, et al., 2018, Martin
144 and Schlüter, 2015) - and traditional discrete event simulation that employs a top-
145 down, process-oriented modelling approach (Siebers, et al., 2010, Bonabeau, 2002).
146 The choice to use ABM is to allow for the exploration of a variety of scenarios related
147 to the hydrology and sediment processes, but is primarily intended to allow for future
148 expansion of the model to incorporate more complex human-environment
149 interactions such as farmer decision making. Whilst this paper is focused on an
150 archaeological example, the techniques employed have the potential to contribute to
151 studies of the efficacy and sustainability of sediment-trap systems in the modern
152 world by providing information on the accumulation of sediments over centuries,
153 rather than simply over the few years available to modern observational studies
154 (Barton, 2016).

155

156 **2. Study Area and Archaeological Background**

157 Engaruka provides an opportunity to study sediment-transport and accumulation
158 processes over long temporal scales which would otherwise be difficult in modern
159 extant agricultural systems. The site is located in the East African Rift Valley, is
160 centred at 2 59' 20" S, 35° 57' 45"E, and the former field area slopes from west to
161 east from c. 1000 m asl to c. 850 m asl (Fig. 1). The system of irrigated agricultural
162 fields at Engaruka was abandoned by the 19th century CE, covers approximately
163 20 km², and comprises an extensive network of irrigation channels, stone-bound
164 fields, agricultural terraces and sediment traps (Westerberg, et al., 2010, Stump,
165 2006, Sutton, 1978). The abandoned field system has been categorised into three
166 distinct sections of the North, Central and South Fields (Sutton, 1998) (Fig. 1) based
167 on differences in field construction, with the majority of the North Fields and parts of
168 the South Fields constructed through periodic sediment capture and accumulation,
169 while the Central fields were built by tilling the existing topsoil and removing stones
170 from the field area (Lang and Stump, 2017, Stump, 2006).



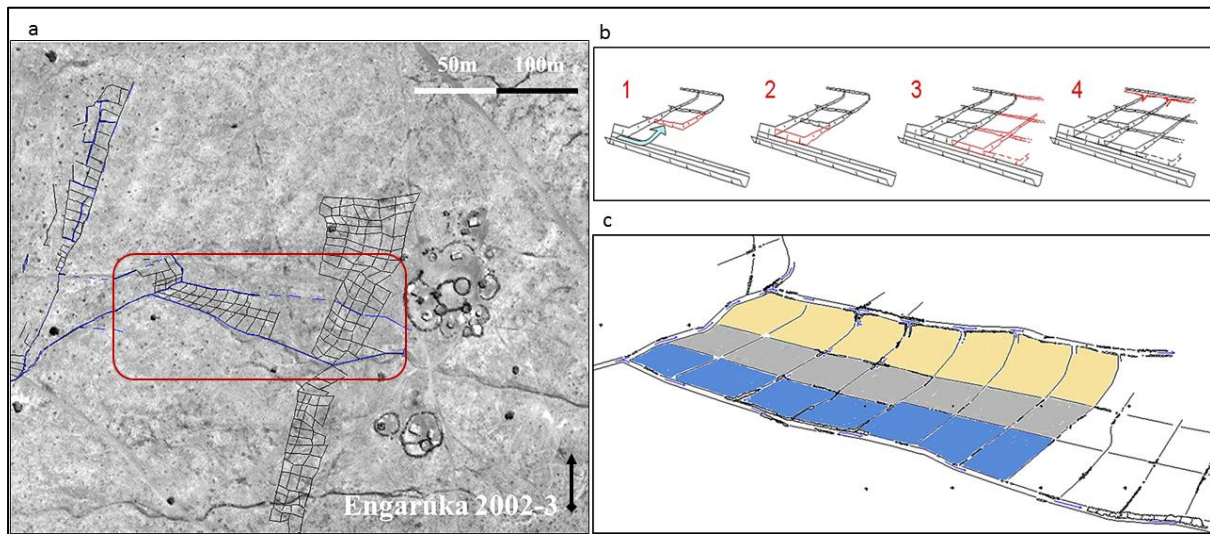
172

173 Figure 1: Location of Engaruka and extent of the agricultural field system, showing
 174 river sources and village settlements (Laulumaa, 2006, Sutton, 1978). Source of
 175 regional map: National Geographic World Map (Esri, 2011). Copyright © Esri.

176

177 Detailed stratigraphic excavations (Stump, 2006) and a combination of stratigraphy,
 178 geochemistry and soil micromorphology (Lang and Stump, 2017) have demonstrated
 179 how sediments were accumulated. The results of excavations and surveys
 180 undertaken in the North Fields area of Engaruka in 2002-3, reported in Stump
 181 (2006), demonstrated that fields in this area were constructed by building a series of
 182 c. 6 × 6 m L-shaped drystone walls, with each new L-shaped wall forming a roughly
 183 square field by abutting earlier walls built in the same manner (Fig. 2b). The water
 184 and sediments supplied to this block of fields were transported from the main river
 185 Engaruka by the primary irrigation furrows (Fig. 1) which then branched off into the
 186 smaller canalised streams and irrigation canals (Fig 2a) that distributed water and
 187 sediments into the blocks of fields. The individual fields within the block are

188 interconnected by a series of smaller channels that allow distribution of water and
189 sediment between the fields and excess runs off into the canalised stream (Fig 2c).
190



191
192 Figure 2: a) Location of the block of fields being modelled (within the red bounding
193 box), the blue lines indicate the water channels and canals that surround a block of 6
194 x 6 m drystone-bound fields; b) Phases of field construction based on excavations of
195 part of the North Fields (Stump, 2006); c) Plan of the group of sediment trap fields
196 and associated water channels in the North Fields section of Engaruka used to
197 simulate the field system in the ESTTraP model, based on excavations conducted by
198 Stump (2006) . Interpretation of stratigraphic data suggests that the fields were
199 constructed consecutively from the upper fields (yellow) through the middle fields
200 (grey) and down to the lower fields (blue), and from left to right (i.e. from upslope to
201 downslope).

202 There are, however, limitations to these stratigraphic data that in turn limit our ability
203 to employ them to address broader issues regarded the development and
204 management of the agricultural system. The first of these - that these data
205 demonstrate the sequence and manner of field construction but provide no
206 information on the time it took to build an individual field or group of fields - has been
207 highlighted already. A second limitation requires a little more explanation, and arises
208 from the fact that it is often difficult or impossible to discern on purely stratigraphic
209 grounds whether irrigation channels, canals or ditches were built in one construction
210 episode or through successive phases of construction; an issue most commonly
211 discussed in terms of identifying maintenance of structures or differentiating

212 maintenance from modification (Doolittle, 2015, Howard, 1993, Doolittle, 1984). To
213 illustrate this in the case of Engaruka, note that the alluvial sediments captured
214 within the fields could be delivered by water transported within the canalised stream
215 (as shown in Fig. 2b, phase 1), with the stratigraphically later canal employed solely
216 to deliver water for irrigation after these fields had been constructed (as shown in
217 Fig. 2b, phase 4). Alternatively, it is equally possible that sediments were
218 transported within the smaller irrigation canal, as suggested by observations and
219 conversations with farmers in Konso, Ethiopia, who build analogous sediment traps
220 by first diverting stream-flows along small canals (see Ferro-Vázquez, et al., 2017).
221 Deciding between these two scenarios cannot be achieved based on the
222 stratigraphic data alone, since the canal shown in Fig. 2b phase 4 could have been
223 periodically extended: i.e. the stratigraphic evidence merely demonstrates that the
224 ditch and drystone lining to this canal were inserted later than the field walls and
225 captured sediments they truncate, not that the whole canal was built in a single
226 construction episode. The construction sequence presented in Stump (2006) and
227 summarised in Fig. 2b was thus based on the interpretative inference that collecting
228 sediments entrained within comparatively small canals would take too long to be of
229 practical benefit to farmers. Without data on possible sediment accumulation rates
230 the interpretation of the sequence of field construction is merely an assumption.

231

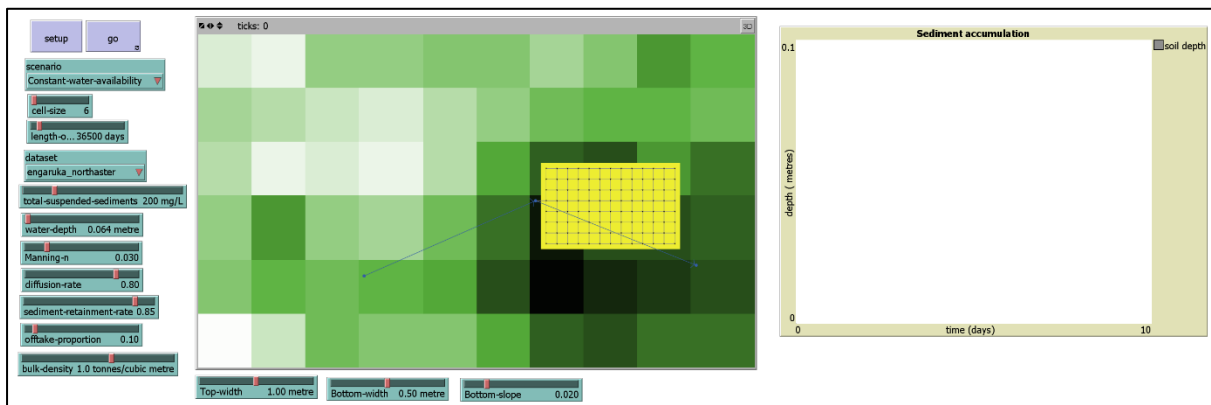
232 The recognition that subtly different processes could produce the same sequence of
233 field construction requires a method of investigating whether sediments were
234 accumulated quickly during relatively large flood events or more slowly via the
235 control of flows within small irrigation canals. One such approach is the use of ABM
236 techniques since they can both explore the multitude of interacting hydrological and
237 sedimentological factors involved and can investigate the effects of different
238 scenarios such as changes to vegetation or climatic conditions. By modelling how
239 water flowed through the irrigation channels, it is possible to assess how much
240 entrained sediment could be transported, and therefore extrapolate the amount of
241 sediment that can be accumulated and the rates at which these sediment traps could
242 be constructed and expanded over time.

243

244 **3. Materials and Methods**

245 **3.1 Engaruka Sediment Transport and Trapping (ESTTraP) Model Overview**
246 **and Framework**

247 The ESTTraP model is implemented in the NetLogo platform version 5.2.1
248 (Wilensky, 1999) and its documentation is based on the ODD+ protocol (Müller, et
249 al., 2013, Grimm, et al., 2006). In this implementation of the model, a block of 90
250 individual stone-bound fields were modelled to understand the timescales and
251 pattern of sediment accumulation given simulated scenarios of different
252 environmental conditions. Using a georeferenced digital elevation model to build the
253 model environment, the ASTER GDEM V2 (NASA_LP_DAAC, 2011) was resampled
254 using the nearest neighbour interpolation technique from the original 30 m resolution
255 to a resolution of 6 m to match the size of the stone-bound fields recorded from
256 excavations within the North Fields (Stump, 2006). Each field within the model thus
257 has a 6 x 6 m resolution (Fig. 2 and Fig.3), with sediment accumulation simulated for
258 a block of 90 such fields covering approximately 3,000 m² of the c. 9 km² North
259 Fields area of Engaruka (Fig. 1).
260



261
262 Figure 3: ESTTraP model interface showing the modelled block of fields (yellow)
263 connected by a network of canals.

264 Excavation evidence shows that the process of accumulating sediments acted to
265 level slight variations in slope of the pre-existing topography. This is clearest in the
266 fields constructed adjacent to the canalised stream where up to 700mm of sediments
267 were captured on their downslope side with as little as 100 mm towards their upslope
268 extent, resulting in a wedge shape of captured sediments (Stump, 2006). This
269 pattern of sediment accumulation allowed for sloping land to be levelled for improved

270 agricultural production. The sediment depth of 700 mm across the block of 90 fields
271 therefore represents a maximal depth of accumulated deposits with the assumption
272 that the fields are of equal dimensions and that the excavated examples are broadly
273 representative of other fields in this area. For the purposes of the current modelling
274 process we have therefore taken 350 mm as an average depth of sediment
275 accumulation, i.e. approximately half of the maximal average depth of 700 mm to
276 account for this wedge shape.

277

278 The hydrological and sediment-transport model is implemented through agents
279 consisting of a network of nodes and directional links to represent the irrigation
280 channels that transport water and sediments to the fields. The nodes contain
281 information on the flow and sediment discharges along the system of canalised
282 stream and irrigation channels based on the agent characteristics. The directed links
283 that represent the irrigation channels distribute water and sediments from the
284 canalised stream into the fields via nodes set within each 6 x 6 m field. At each
285 model time step (representing a day) each node shares a percentage of its amount
286 of sediments and water equally with its neighbours in the network of nodes. The
287 nodes also retain a percentage of the sediments and water flows to represent
288 sediment and diffusion loss incurred as these agents move along the network.
289 Sediments and water flows terminate at the fields, where the nodes transfer these
290 agents to the field patches as sediment discharge, which is then converted to
291 represent sediment accumulation (Appendix A.3).

292 The model runs on a daily time step with 365 steps per year, and with data collected
293 at each time step on the amount of sediment accumulated and changes in sediment
294 depth. At each time step agents perform the following actions (which represent the
295 sub-models of the ESTTraP ABM):

296

297 1) Generation of water flows: the estimation of flow rates and discharge from the
298 irrigation channels is based on Manning's equation for open-channel continuous
299 flows for trapezoidal channels (Robert, 2014, 31):

$$300 \quad Q = \frac{k}{n} (R)^{\frac{2}{3}} \sqrt{S} A \quad (1)$$

301 Q represents water discharge ($\text{m}^3 \text{s}^{-1}$) from the irrigation channels, k is a
302 dimensionless constant (=1 for SI units), n is the Manning's roughness coefficient; R

303 represents the hydraulic radius (m); S represents the slope of the channel (m m^{-1}),
 304 and A is the cross-sectional area of the channel (m^2). The water is then transported
 305 and distributed to the canals and fields. The dimensions of the canals are based on
 306 archaeological data from excavations (2006), where a canal top-width of 1.0 m and
 307 canal bottom-width of 0.5 m (Appendix A) are used to estimate the hydraulic radius
 308 and cross-sectional area of the canal. On the basis of excavated examples, the total
 309 depth of canals (as opposed to channels and canalised streams) rarely exceeds 300
 310 mm, but water depths and hence the wetted perimeter of canals is more important
 311 factors than the maximum physical depth of a canal. Simulated water-depths
 312 (section 3.2 below), in conjunction with these dimensions, are thus used to
 313 determine discharge.

314

315 2) Sediment transport and discharge: sediments are transported by water in the
 316 irrigation channels, with the model focused on sediments transported in suspension
 317 and discharged into the fields based on the following relationship (Van Rijn, 1993):

$$318 \quad Q_s = Y C_t Q \quad (2)$$

319 Q_s represents sediment discharge (tonnes day^{-1}) into the fields. Q represents water
 320 discharge (m^3s^{-1}), C_t is the daily total suspended sediment (mg L^{-1}) and Y is a
 321 conversion factor that converts $\text{m}^3 \text{s}^{-1}$ to $\text{m}^3 \text{day}^{-1}$ and mg L^{-1} to tonnes m^{-3} .

322 Entrainment and re-entrainment of sediments in the canals is considered to be
 323 minimal as the canals modelled are stone-lined and relatively smooth, and thus
 324 representing the daily sediment as a constant, average value is reasonable.

325

326 3) Sediment accumulation in the fields: sediments discharged into the field then
 327 accumulate as a function of the sediment discharge and the bulk density of the
 328 sediments, constrained by a soil compaction factor (van Rijn, 2013, Wilkinson, et al.,
 329 2006, 7):

$$330 \quad \Delta H_i = \frac{\Delta S_{tot,i}}{f_i} \quad (3)$$

331 Where:

$$332 \quad \Delta S_{tot,i} = \frac{Q_{s,i}}{BD} C \quad (4)$$

333 ΔH_i represents the depositional layer thickness (m), $\Delta S_{tot,i}$ represents the total
334 sediment volume in a given stone-bound field i ($\text{m}^3 \text{ day}^{-1}$), f_i is the area of a given
335 stone-bound field i (m^2), $Q_{s,i}$ is the sediment discharge within a given stone-bound
336 field i (tonnes day^{-1}), BD is the bulk density of the soil (for clays such as at Engaruka,
337 $1.0 - 1.6 \text{ tonnes m}^{-3}$) (McKenzie, et al., 2002, FAO, 2006, 51), and C is a
338 consolidation/compaction rate of deposited sediment ($1 / \text{days}$).

339

340 The model design assumes 100% sediment trap efficiency, whereby all sediments
341 discharged into the fields were captured and accumulated within those fields, which
342 is not unreasonable given the geometry of the surface and stone walls. Total
343 suspended sediments (TSS) were kept constant at 200 mg L^{-1} , and the data values
344 for TSS of c. 200 mg L^{-1} and the water depth of 0.1 m were selected based on a
345 hydrological study conducted in 2015 along a 4 km section of the Engaruka River
346 (Fig. 1). These instrumental measurements are not unreasonable in the long term
347 when reviewed in conjunction with CRUTS data (Harris, et al., 2014) on the rainfall
348 and temperatures for the region and provide baseline approximations since the
349 system is now abandoned. The choice of water depth is further supported by the
350 results of the sensitivity analyses which found that water depths greater than 0.5 m
351 would result in increased water discharge, which could potentially damage the
352 channel walls by eroding their surfaces (Appendix B).

353

354 **3.2 Model Simulations and Scenarios**

355 Global sensitivity analysis (Thiele, et al., 2014, Saltelli, et al., 2008) was conducted
356 on the model parameters for water depth, TSS and Manning's n to explore model
357 behaviour and the influence of model parameters on outputs (Appendix B). The
358 model was then implemented using a series of four scenarios to try to understand
359 how the environmental factor of rainfall availability and variability, represented by
360 water depth, would influence water and sediment discharge and thus sediment
361 accumulation. The four scenarios simulated in the model are: SIM-01 Constant water
362 availability, SIM-02 Seasonal variability, SIM-03 Long-term climate variability, and
363 SIM-04 Vegetation cover impact. The scenarios modelled are about end-members,
364 i.e. the diverse unimodal grain-size populations of sediments that are the result of
365 different erosive processes (Seidel and Hlawitschka, 2015), and are intended to
366 constrain sediment-transport rates rather than being realistic representations of the

367 compositional aspects of sediment-transport processes. The implementation of
368 these four scenarios would help define the timescales involved in accumulating
369 sediments within the field system. Simulations were run for a period of 100 years at a
370 daily time-step to incorporate multi-decadal variability in climate conditions. Model
371 uncertainty was assessed using Monte Carlo simulation of runs whereby the model
372 scenarios were simulated over 100 replicated runs to estimate the distribution of
373 model outputs.

374

375 **SIM-01 Constant water availability:** idealised conditions of constant water
376 availability over time, which are intended to characterise an end-member of potential
377 system behaviour, are represented by a constant water depth of 0.1 m based on
378 observations of water-depths conducted during field survey along a 4 km stretch of
379 the Engaruka River and modern irrigation channels in 2015.

380 **SIM-02 Seasonal variability:** the climate in Engaruka follows a bimodal rainfall
381 pattern during a calendar year with two wet seasons interspersed with two dry
382 seasons (Jones and Harris, 2008, Ryner, et al., 2008). The seasonal variability was
383 simulated in the model by increasing and decreasing the constant water depth of 0.1
384 m by 20% to represent seasonal fluctuations in water availability. The 20% was an
385 estimated range based on observations of the highest and lowest values of water
386 depth from the observations made in 2015.

387 **SIM-03 Long-term climate variability:** in combination with seasonal variability,
388 longer term climate variability is also evident within the East African region. Studies
389 of palaeoclimatic proxies (Marchant, et al., 2018, e.g. Westerberg, et al., 2010, 305,
390 Ryner, et al., 2008, Barker and Gasse, 2003, Verschuren, et al., 2000) suggest that
391 over the last 1,100 years the East African region has experienced warm and wet
392 climates interspersed with long periods of drought at a decadal scale. The longer-
393 term variability was simulated by increasing or decreasing the average annual water
394 depth and intra-annual seasonal variability by 20% over decadal scales to simulate
395 long dry or wet periods, which means that in this simulation the baseline flows are
396 shifted up and down by 20% at a decadal scale and within that seasonal variability
397 increases and decreases by 20% of the decadal baselines .

398 **SIM-04 Vegetation cover impact:** in combination with seasonal variability, the
399 vegetation cover of a landscape also influences water-discharge rates with runoff
400 increasing by approximately 30% on bare ground as compared to areas with

401 vegetation cover (Lesschen, et al., 2009). One of the possible outcomes of reduced
402 vegetation cover would be increased surface runoff during rainfall events which
403 could possibly result in increased water depth and elevated levels of entrained
404 sediments in the channels.

405

406 The scenarios modelled are intended to explore how the differences in water
407 availability over time (which is a factor of seasonal and long-term climate fluctuations
408 and vegetation cover) influenced sediment accumulation within the sediment trap
409 fields and thus field construction and expansion.

410

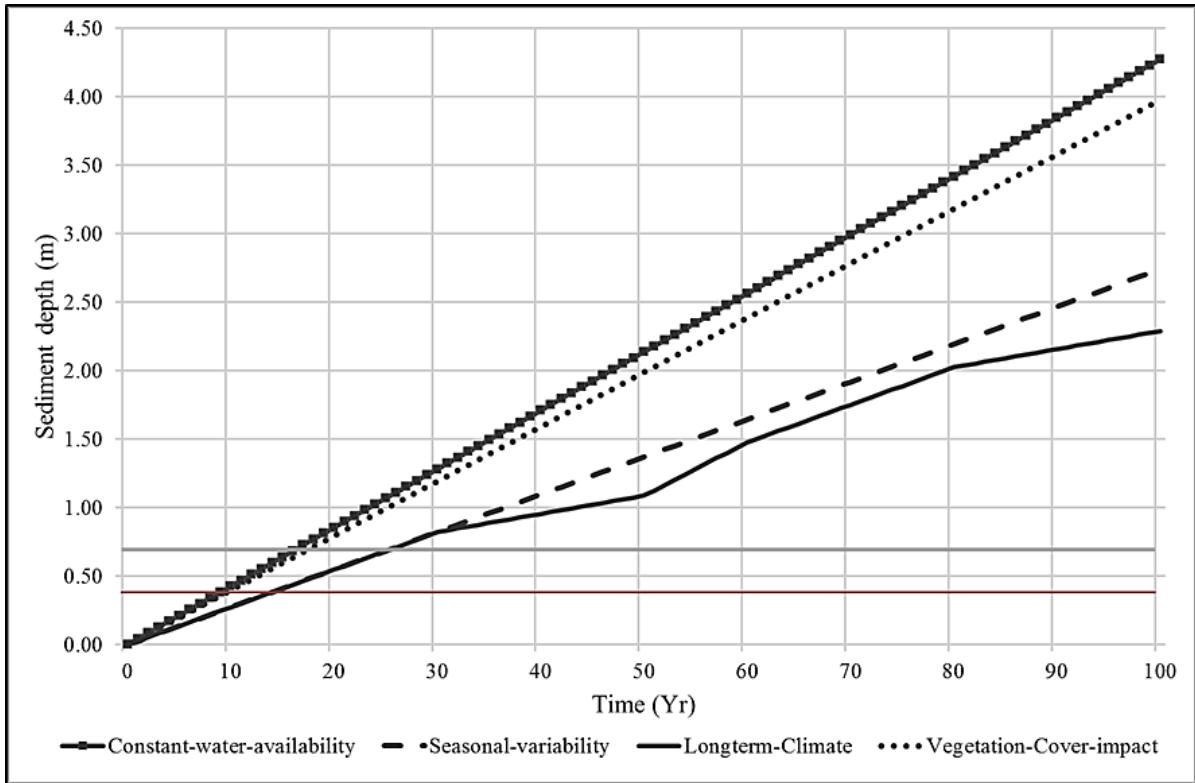
411 **4. Results**

412 Results of the sensitivity analyses show that sediment discharge can be interpolated
413 from water discharge and that the model simulates this function as expected, such
414 that as water discharge increases sediment discharge also increases. Sediment
415 discharge is a linear function of water and TSS, and increases in the water depth
416 values would therefore result in increases in the sediment discharged and therefore
417 the accumulation rates in the fields (Appendix B). This approximation has
418 implications for the results of the scenarios modelled in that the sediment discharge
419 and consequent accumulation would be affected by the water depths simulated to
420 represent the variability in water availability due to climate conditions. Relative to the
421 variation of the model parameters, the uncertainty analyses show that the scenarios
422 for climate variations that would result in variations in water availability play a role in
423 sediment accumulation (Appendix B).

424

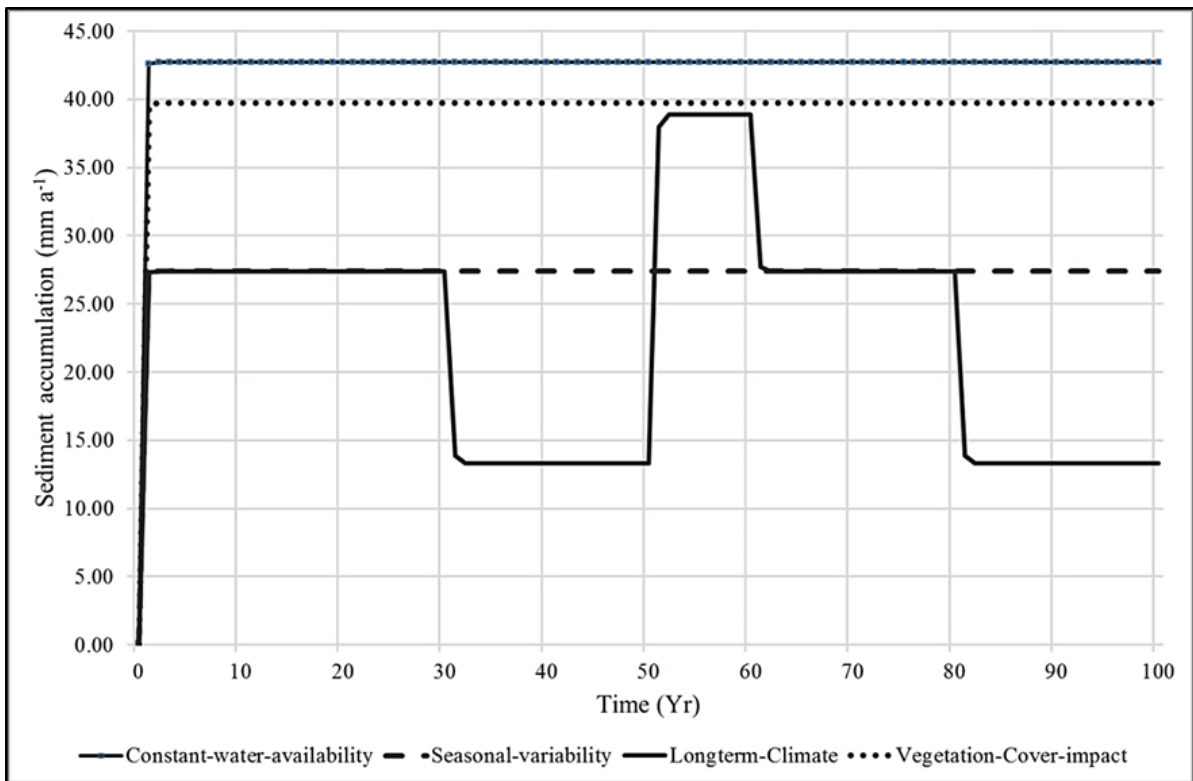
425 The results of the model simulations provide information on the amount of time and
426 rates at which sediments accumulate within the entire block of 90 fields. The four
427 scenarios of constant water availability (SIM-01), seasonal variability (SIM-02), long-
428 term climate variability (SIM-03), and vegetation cover impact (SIM-04) were
429 simulated for a period of 100 years at a daily time-step to see how long it would take
430 to accumulate sediments to the observed depths of 350 mm (Fig. 4). It would
431 therefore take a shorter time to accumulate sediments, with sediments accumulating
432 to a depth of 350 mm across the 3,000 m² block of 90 fields after 8 years for
433 conditions modelled in SIM-01 and SIM-04, and 13 years for SIM-02 and SIM-03
434 (Fig. 4). Given that it would take 8 – 13 years to accumulate sediments across the

435 block of fields, it would take approximately 1 – 2 months to build each 6 x 6 m field
 436 individually. This range of estimates from the model end-members provides a
 437 maximum and minimum time scale for the development of the fields.
 438



439
 440 Figure 4: Mean annual cumulative sediment depth (metres) for a block of 90, 6 × 6
 441 metre stone-bound fields based on simulations for four scenarios of constant water
 442 availability (SIM-01), seasonal variability (SIM-02), long-term climate variability (SIM-
 443 03), and vegetation cover impact (SIM-04) over a period of 100 years. The horizontal
 444 grey line highlights the sediment depth of 700 mm and the red line highlights
 445 sediment depths of 350 mm corresponding to those observed from the
 446 archaeological excavations.

447



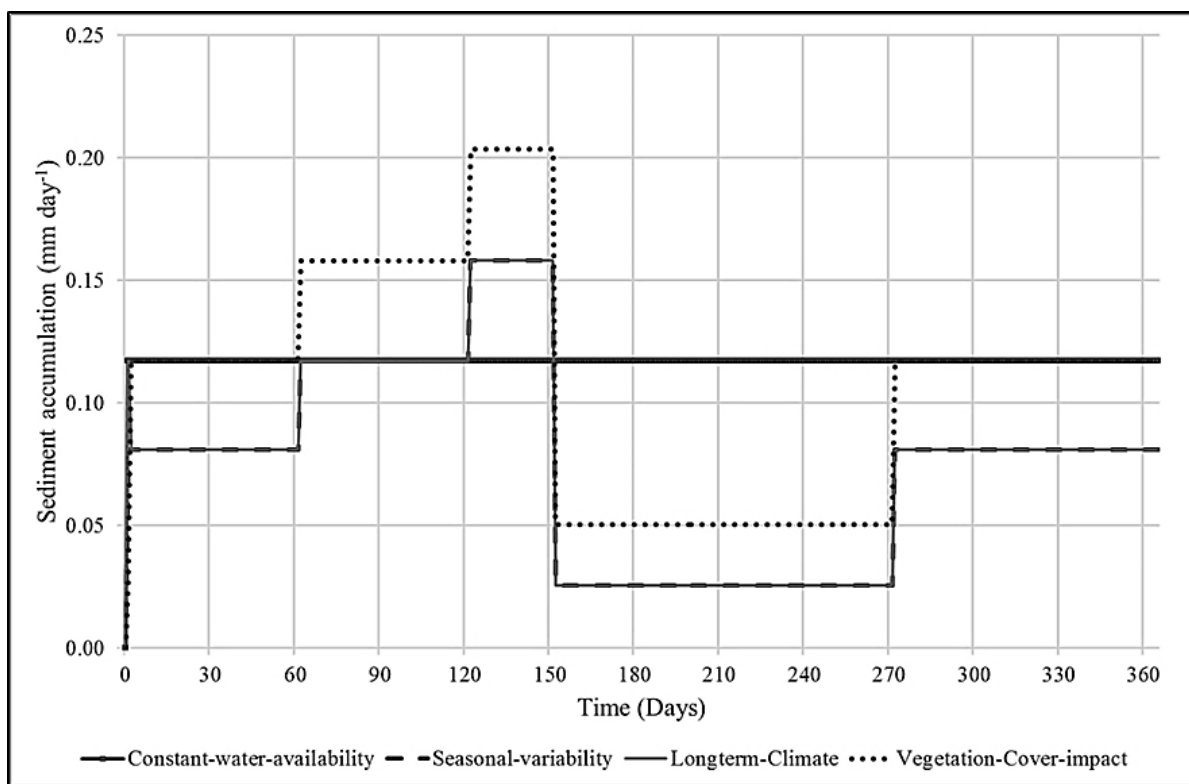
448

449 Figure 5: Mean annual sediment accumulation rates (mm a⁻¹) modelled for the four
 450 scenarios of constant water availability (SIM-01), seasonal variability (SIM-02), long-
 451 term climate variability (SIM-03), and vegetation cover impact (SIM-04) for a block of
 452 90 fields over a period of 100 years.

453 Looking at the average annual rates of sediment accumulation for a block of 90 fields
 454 (Fig. 5), SIM-01 had the highest rates at 42 mm a⁻¹, followed by SIM-04 at 39 mm a⁻¹
 455 and SIM-02 at 27 mm a⁻¹. Longer term variations in climate account for the
 456 fluctuations in sediment accumulation rates seen in SIM-03, ranging from 38 mm a⁻¹
 457 during the much wetter periods, to as low as 13 mm a⁻¹ during the periods simulated
 458 for extreme dry conditions, and an average of 22 mm a⁻¹ over the 100 years. This
 459 lower mean annual sediment accumulation rate of 22 mm a⁻¹ means that it could
 460 have taken 16 years for sediment depths to reach 350 mm across the 3,000 m²
 461 block of 90 fields. The prolonged dry conditions simulated in SIM-03 were set to
 462 have a minimum water depth that would simulate low water availability but not the
 463 complete absence of water. This scenario is based on evidence that the perennial
 464 Engaruka River was one of the water sources for the irrigation channels in the North
 465 Fields (Stump, 2006, Sutton, 1998), meaning that water supply to the fields would
 466 have still been possible but the amount of water in the channels would most probably
 467 have been greatly reduced.

468

469 Although the annual sediment accumulation rates presented in Fig. 5 appear to be
470 constant when averaged out for each year; these rates do not reflect seasonal
471 fluctuations in water availability that would affect sediment discharge and
472 accumulation within the fields. The influence of seasonal variability on sediment
473 accumulation was therefore explored further to see how these intra-annual/daily
474 fluctuations influence sediment accumulation rates (Fig. 6 and Fig. 7). It should be
475 noted that there is no simulation for intra-daily variability as the model assumes
476 shorter timescale variability averages out for the purposes of this study.
477

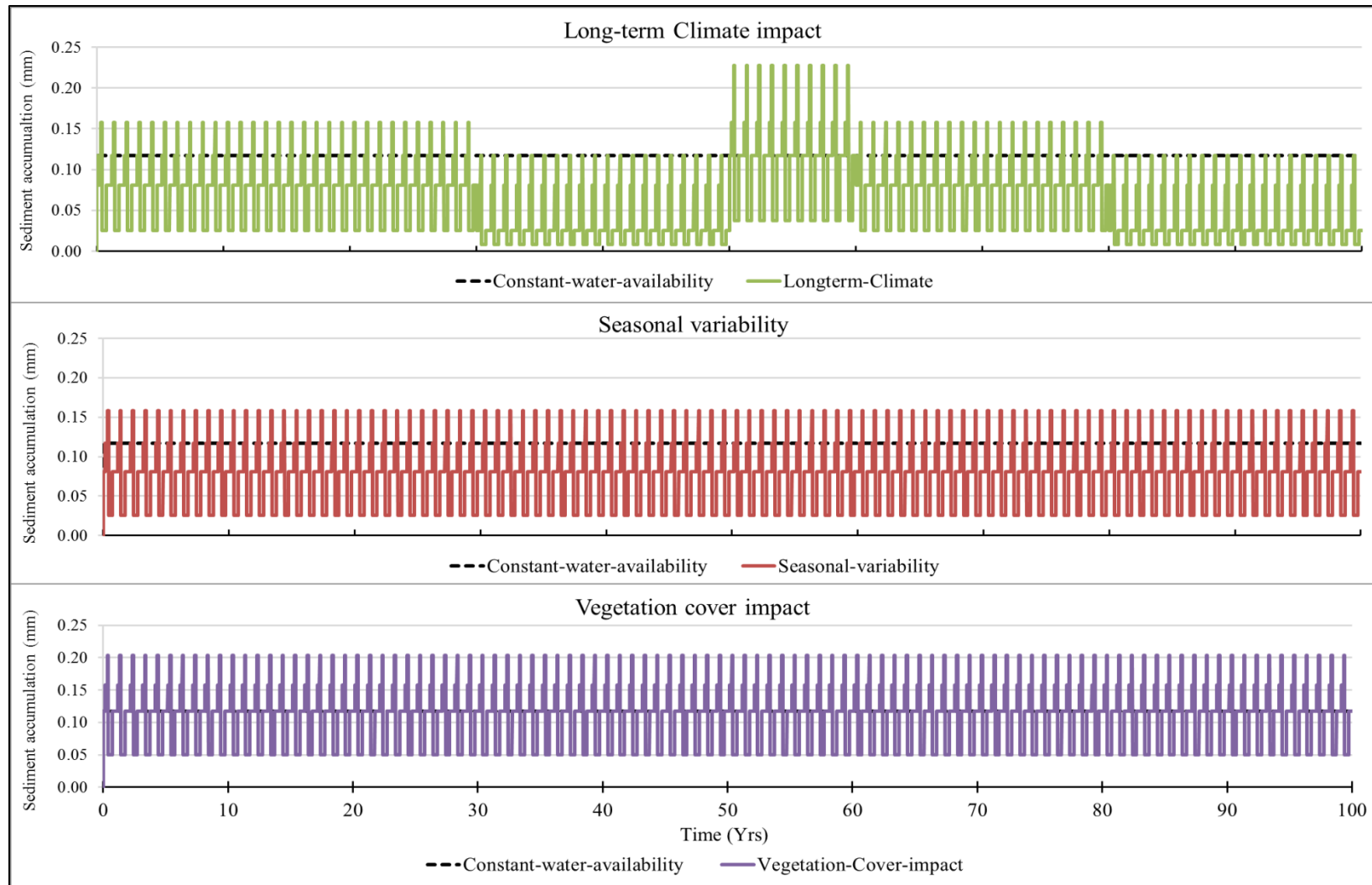


478

479 Figure 6: Intra-annual/daily sediment accumulation rates (mm day⁻¹) show the
480 variations in sediment accumulation over a one year period i.e. Year 1 of the model
481 for scenarios of constant water availability (SIM-01), seasonal variability (SIM-02),
482 long-term climate variability (SIM-03), and vegetation cover impact (SIM-04).

483 As shown in Fig. 6, for SIM-02 and SIM-03 the average daily sediment accumulation
484 rates ranged from 0.03 mm day⁻¹ during the dry seasons to 0.16 mm day⁻¹ during the
485 rainy seasons, while the daily rates for SIM-04 ranged from 0.05 mm day⁻¹ in the dry
486 season to 0.20 mm day⁻¹ in the rainy seasons. This result is in contrast to SIM-01
487 where the daily rates throughout the year were constant at 0.12 mm day⁻¹.

488 Simulations for long-term climate variability combined with seasonality (SIM-03) had
489 the greatest impact on the sediment accumulation within the fields, with scenarios
490 suggesting that it would take 13 years to accumulate 350 mm of sediments across
491 the block of 90 fields (Fig. 4). However, over the longer timescales of the 100-year
492 period (Fig. 7) these seasonal fluctuations varied further based on extremes of
493 drought or wetter conditions. When extreme dry conditions were simulated between
494 Year 30 - 50 and Year 80 – 100, these sediment accumulation rates dropped to 0.01
495 mm day⁻¹ during the dry seasons and were highest at 0.12 mm day⁻¹ during the rainy
496 seasons. In the wetter periods simulated between Year 50 - 60, these sediment-
497 accumulation rates were 0.04 mm day⁻¹ during the dry seasons and rose to 0.23 mm
498 day⁻¹ during the rainy seasons (Fig. 7). These periods of extreme weather had a
499 marked effect on sediment depth within the block of fields with the average depth at
500 2.30 m after the 100-year period, the lowest of all the simulations. The results of
501 these climate-variability scenarios mean that if farmers attempted to accumulate
502 sufficient sediments to fill these fields to the 350 mm depths observed
503 archaeologically during a comparatively wet period the fields could be filled in 9
504 years, but attempts to do the same during the conditions that prevailed during the dry
505 period would take 27 years.
506



507

508 Figure 7: Daily sediment accumulation rates (mm day⁻¹) simulated for scenarios of constant water availability (SIM-01), seasonal variability
 509 (SIM-02), long-term climate variability (SIM-03), and vegetation cover impact (SIM-04) over a period of 100 years.

510 The low or no vegetation cover in the catchment simulated for in SIM-04 would result
511 in higher surface runoff and water influx into the channels. This would then result in
512 higher discharge rates and thus higher sediment accumulation rates within the fields
513 such that SIM-04 resulted in high annual sediment accumulation rates at 39 mm a^{-1}
514 (Fig. 5). The block of fields took an average of 9 years to accumulate sediments to a
515 depth of 350 mm across the c. $3,000 \text{ m}^2$ block of 90 fields. These high rates of
516 sediment accumulation could also be seen in the daily rates for SIM-04, ranging from
517 0.05 mm day^{-1} in the dry season to $0.12 - 0.16 \text{ mm day}^{-1}$ and then rising to 0.20 mm
518 day^{-1} in the rainy seasons (Fig. 6 and Fig. 7). SIM-04 presents a case that takes into
519 consideration the removal of vegetation cover from the upslope catchment areas that
520 could result in increased surface runoff in the short term. In addition, the possible
521 removal of forest vegetation cover on the hillslopes upstream of the agricultural fields
522 is likely to have affected water availability over the longer-term in both dry and rainy
523 seasons, with the loss of vegetation and soil reducing the water holding capacity
524 within the upland river catchments.

525

526 **5. Water availability, sediment accumulation and field development**

527 The four scenarios influencing water availability explored in the model present
528 important steps in understanding the temporal scales and patterns of field
529 development that resulted in the expansion of the Engaruka water-management
530 system. As discussed in Section 1 and 2 above, the excavations of the site show that
531 the construction of the drystone-bound fields was tied to sediment accumulation. The
532 farmers would lay a few courses of the drystone walls and as the sediments
533 accumulated behind these drystone walls the farmers could add further courses
534 when needed, thus construction of the wall courses and the sediment trap fields
535 were tied to the rate of sediment accumulation. The scenarios discussed above point
536 to the influence of variability in water availability on the construction and
537 development of a block of fields and the timescales involved. This variability relates
538 to both seasonal and long-term climate changes that affected the east African region
539 (Marchant, et al., 2018); and by focusing on specific aspects of water availability, we
540 can use this information to understand the patterns of sediment accumulation and
541 field construction that influenced the development of the Engaruka system.
542 Understanding the impacts of seasonality, climate variability and vegetation cover on
543 the availability of water and sediment accumulation helps support interpretations of

544 the archaeological evidence by providing additional data to refine stratigraphic
545 interpretations of the timelines and patterns involved in the development of the field
546 systems.

547

548 The block of 90 fields simulated in the model took between 8 to 13 years, and up to
549 27 years during prolonged dry conditions, to accumulate sediments to a depth of 350
550 mm, given differing scenarios of water availability for sediment transport. At a finer
551 resolution it would take individual 6 x 6 m fields between 1 - 2 months when flows
552 are occurring to accumulate sediments to depths of 350 mm and the farmers would
553 be able to add one or two courses to the drystone walls with the sediments
554 accumulating behind these wall courses. This means that farmers can construct
555 individual fields within a field block over a period of a single cropping/growing season
556 and continue to add wall courses and expand field construction across the block of
557 fields. The timescales presented by this model are best estimates of average
558 conditions for sediment accumulation and field construction. The model results
559 suggest that the fields could have been developed by utilising low flows of water in
560 irrigation canals to transport and accumulate sediments in small fields over
561 successive seasons, and thus do not require the larger flooding events from
562 overbanking or diverted streams envisaged by Stump (2006).

563

564 The amount of time it would take to accumulate 350 mm of sediments within a block
565 of fields also points to concurrent construction of multiple blocks of fields across the
566 entire Northern Fields areas rather than the consecutive construction of field blocks;
567 an interpretation suggested by Stump (2006) on the basis of stratigraphic data and
568 the interpretation of field layouts in relation to water courses, but one which remained
569 speculative without approximations of sediment accumulation rates. Given model
570 results suggesting 8 - 13 years to construct a block of 90 fields covering 3,000 m², it
571 would take between 24,000 - 39,000 years to construct the fields across the entire 9
572 km² of the North Fields if the field blocks were constructed sequentially. These time
573 scales are clearly far beyond the time periods in which Engaruka was in use. Indeed,
574 the North Fields area only forms part of the entire 20 km² field system, with
575 accumulated sediment depths in the South Field area up to 2.0 m deep (Lang and
576 Stump, 2017), making it unlikely that the society in the Engarukan system widely
577 relied on sequential field construction. If the ESTTraP model results hold true for

578 real-world scenarios, multiple blocks of fields must have been constructed
579 concurrently across the North Field sections, and it is possible that the North Field
580 and South Fields areas of the site were also constructed simultaneously. This
581 interpretation in turn has implications for discussions of social hierarchy and
582 resource management, as it suggests individual farmers, households or extended
583 families (such as clans) could have built the extensive field remains and irrigation
584 network without the need for central control or long-term planning, with each block of
585 fields constructed and managed by a small group of individuals.

586

587 The ESTTraP model demonstrates the utility of agent-based modelling to assess the
588 sediment transport dynamics and their influence on sediment accumulation and
589 patterns of field construction. For example, although the results presented here
590 suggest that farmers could utilise low flows of water to transport and accumulate
591 sediments in the small individual 6 x 6 m plots evidenced in the North Fields, it is
592 possible that much higher flows were employed to accumulate sediments quickly in
593 the much larger fields located towards the south of the site (see Lang and Stump,
594 2017). This manipulation of the amounts of water flowing would influence not only
595 the spatial scales but the temporal scales for the development of the field system as
596 well as the choice of consecutive or concurrent field construction. However, there
597 would nevertheless be limitations to this where diversion of water and sediment to
598 multiple field blocks would limit the flow available to each plot. The construction of
599 field blocks simultaneously would thus require water resources to be shared between
600 the groups constructing each new block or irrigating existing plots, which would have
601 further implications on water availability and the attendant water and sediment
602 discharge capacity. This would also raise questions on the management of these
603 water resources as issues of competition for water resources may arise among
604 farmers, particularly when water flows are low during extended dry periods. These
605 aspects of water sharing and competition are being further explored in versions of
606 the ABM that assess the effect of concurrent field construction and which
607 incorporates human agents within the simulated landscape.

608

609 **6. Conclusions**

610 The ESTTraP model demonstrates an ability to model sediment accumulation rates
611 at the abandoned agricultural site of Engaruka, Tanzania, and given reasonable

612 model parameter approximations shows that blocks of fields at Engaruka are likely to
613 have been constructed concurrently across the field system rather than sequentially.
614 This conclusion substantially refines previous interpretations of stratigraphic
615 evidence, showing that comparatively low water flows are sufficient to transport
616 sediments that can be captured to create agricultural plots, and thus refutes an
617 earlier interpretation of the stratigraphy of the field system (Stump 2006) that
618 assumed the depths and extent of sediment capture required periodic or controlled
619 flooding events. Field construction could occur over short periods with a single 6 × 6
620 m field taking 1-2 months and a block of 90 fields taking 8 -13 years given constant
621 water flows of as little as 100 mm deep within canals with basal widths of 0.5m.

622

623 Moreover, the results have the potential to be combined with direct dating evidence
624 of fields to refine the site's chronology of construction, and with better dating could
625 be used to relate periods of field construction to palaeoclimatic evidence of changing
626 rainfall regimes. The results of this model thus support arguments by Stump (2016)
627 and Wainwright (2008) on the relevance of combining agent-based models with
628 archaeological data for improved stratigraphic interpretations. The model results
629 support archaeological interpretations where little additional information about the
630 system is available such as direct evidence of water availability and rates of
631 sediment accumulation and field expansion, making this model particularly relevant
632 to other sites and studies for which little or no direct dating evidence is available. The
633 results of these model scenarios would be of particular interest in understanding how
634 other similar agricultural systems developed while taking into consideration the
635 effects of long term climate on water availability.

636

637 Although tailored to a specific archaeological case-study, understanding the rates
638 and patterns of field construction not only has a bearing for the abandoned
639 agricultural site at Engaruka but is of relevance for any archaeological study
640 involving the deliberate or unintended accumulation of alluvial sediments, including
641 the siltation of basins or reservoirs, or the accumulation of sediments within run-off
642 irrigation systems. Even further, knowing the rates and patterns of sedimentation is
643 valuable in estimating alluviation in non-archaeological sites such as modern
644 irrigation systems, whilst the ability to model these process over centennial
645 timescales can aid in the assessment of the legacies of previous land-use and help

646 examine the future sustainability of modern land-use systems. The ESTTraP model
647 thus presents an important resource in the assessment of sediment dynamics and
648 patterns of field development at Engaruka as presented here, but can also be
649 adapted for other archaeological sites and has further applications for modern
650 irrigation systems and future landscape management.

651 **Appendices**

652 **Appendix A: Model Overview**

653 **A.1 Model Assumptions**

654 The ESTTraP agent-based model was constructed to perform a series of simulations
655 to understand the temporal and spatial patterns for the transport and accumulation of
656 sediments within a section of the stone-bound fields in the Engarukan water-
657 management system. This model focuses exclusively on the physical processes of
658 sediment transport and accumulation within a section of the stone-bound fields. The
659 research presented here introduces a model that simulates water flows and
660 sediment transport through a small section of the canal systems and through a c.
661 3,000 m² block of fields in the North Fields section of the site in order to demonstrate
662 the core features of sediment accumulation. The model omits more complex
663 landscape-scale elements: rainfall and surface runoff and erosive processes, as well
664 as site-specific elements of sediment transport such as bedload and saltation. The
665 effects of rainfall and surface runoff on discharge rates are not simulated directly
666 within the model but are simplified and represented by variability in water depth
667 within the irrigation channels. Studies have shown that rainfall increases can lead to
668 an increase in surface runoff which in turn contribute to water flows in channels and
669 canals, correspondingly increasing water depth (Linard, et al., 2009, Montgomery
670 and Buffington, 1998) and resulting in higher water discharge rates. Erosive
671 processes across the landscape are omitted and sediment inclusion is represented
672 by the total suspended sediments in order to focus on sediments already present
673 within the channels. The omission of erosive processes is because the presence of
674 the stone-bound fields across the landscape would act to limit surface runoff and
675 erosion (Mekonnen, et al., 2015, Lesschen, et al., 2009). In addition, the transport of
676 sediments ties closely with the flow rate of water within the channels as the fast
677 moving water will transport larger pebbles while slower flow rates would transport
678 silt, sand and clay (Miedema, 2010, Sundborg, 1956). Studies by Lang and Stump
679

680 (2017) have shown that the sediments captured within the field system were
 681 predominantly clays which tend to be transported in suspension making bedload and
 682 saltation transport processes negligible for this model.

683

684 **A.2 Model Parameterisation**

685 Initial conditions for state variables in each grid cell (elevation in metres above sea
 686 level, soil-depth in metres, and angle of slope) are derived from DEMs,
 687 archaeological excavations and surveys of the study site. The initial values for the
 688 water discharge and sediment discharge vary among simulations; however, some
 689 baselines have been determined based on calibrations from existing data. Baselines
 690 such as water depth, used to determine cross sectional area of the channels, and
 691 total suspended sediments TSS, were based on data from hydrological studies
 692 conducted in 2015 along a 4 km stretch of the Engaruka River. The irrigation channel
 693 dimensions were based on archaeological measurements from studies conducted by
 694 Stump in 2003 in the North Fields of the Engaruka field system (Stump, 2006). The
 695 model parameters, their dimensions and default values are described in Table A. 1
 696 below.

697

698 Table A.1: Model Parameters, variables and Initial values

Parameter	Explanation	Model initial/ default value
Water Transport and Discharge		
Q	Water discharge (m^3s^{-1})	> 0
k	Dimensionless constant	1
n	Manning's roughness coefficient	0.03
R	Hydraulic radius (m)	> 0
S	The slope of the channel (m m^{-1}) i.e. the height difference between the start and end of the channel over the horizontal distance of the channel	0.02
A	Cross-sectional area of the channel (m^2)	> 0
<i>Canal dimensions</i>	Top width	1.0 m
	Bottom width	0.5 m
	Water depth	0.1 m
Sediment Transport and Discharge		
Q_s	Sediment discharge (tonnes day^{-1})	> 0
C_t	Daily total suspended sediment (mg L^{-1})	200

Parameter	Explanation	Model initial/default value
Y	Conversion factor that converts $\text{m}^3 \text{s}^{-1}$ to $\text{m}^3 \text{day}^{-1}$ and mg L^{-1} to tonnes m^{-3}	0.0864
Canal Networks		
CN_jQ	Transport and distribution of water discharge in the network of irrigation canals	> 0
CN_jQ_s	Transport and distribution of sediment discharge in the network of irrigation canals	> 0
w_l	Water discharge loss along the canal network	> 0
d_l	Sediment discharge loss along the network	> 0
t_w	Proportion of water discharge that continues to be transported along the canal networks (%)	0.80
t_d	Proportion of sediment discharge that continues to be transported along the canal networks (%)	0.85
r	Number of irrigation canal recipients in the network	> 0
Sediment Accumulation		
ΔH_i	Depositional layer thickness (m)	> 0
$\Delta S_{tot,i}$	Total sediment volume in a given stone-bound field i ($\text{m}^3 \text{day}^{-1}$)	> 0
f_i	Area of a given stone-bound field i (m^2)	36
$Q_{s,i}$	Sediment discharge within a given stone-bound field i (tonnes day^{-1})	> 0
BD	Bulk density of soils (1g cm^{-3} or 1000kg m^{-3})	1.10 – 1.60
C	Consolidation/compaction rate of soils (days)	365

699

700 **A.3 ESTTraP Model ODD**

701 **A.3.1 ESTTraP Overview**

702 **Purpose**

703 ESTTraP ABM was constructed to perform a series of simulations to understand the
704 temporal and spatial patterns for the transport and accumulation of sediments within
705 a section of the stone-bound fields in the Engarukan water-management system.

706 The purpose of this model is to understand the influence of irrigation infrastructure
707 and water diversion on the accumulation of sediments and development of a series
708 of stone-bound fields in the North fields of the historical irrigation system in
709 Engaruka, Tanzania. Sediment accumulation greatly influences field construction as
710 excavations by Stump (2006) show that as sediments accumulate the farmers place

711 additional drystone courses that over time raise their field walls. In this way, the
712 development of the drystone fields is tied to sediment accumulation.

713

714 **Engaruka North-fields Habitat entities, variables and scales**

715 In this implementation of the model a block of 90 individual stone-bound fields, were
716 modelled to understand the timescales and pattern of sediment accumulation given
717 simulated scenarios of different environmental conditions. Each fields has a 6 × 6 m
718 resolution, and the 90 field block covers approximately 3,000 m² of the 56,000 m² of
719 the simulated landscape. The Engaruka North Fields habitat is characterised by
720 state variables of topography and slope. The habitat is represented by field patches
721 characterised by soil depth and elevation. The fields and irrigation canals are
722 characterised by location and elevation data with the canals further characterised by
723 water velocity generated from analysis of canal dimensions from archaeological
724 excavations. The primary drivers of this model environment are water velocity and
725 suspended sediment volumes within the canalised streams and irrigation canals.
726 Initial conditions for the state variables are described in Appendix A.2 above.

727

728 **Process overview and scheduling**

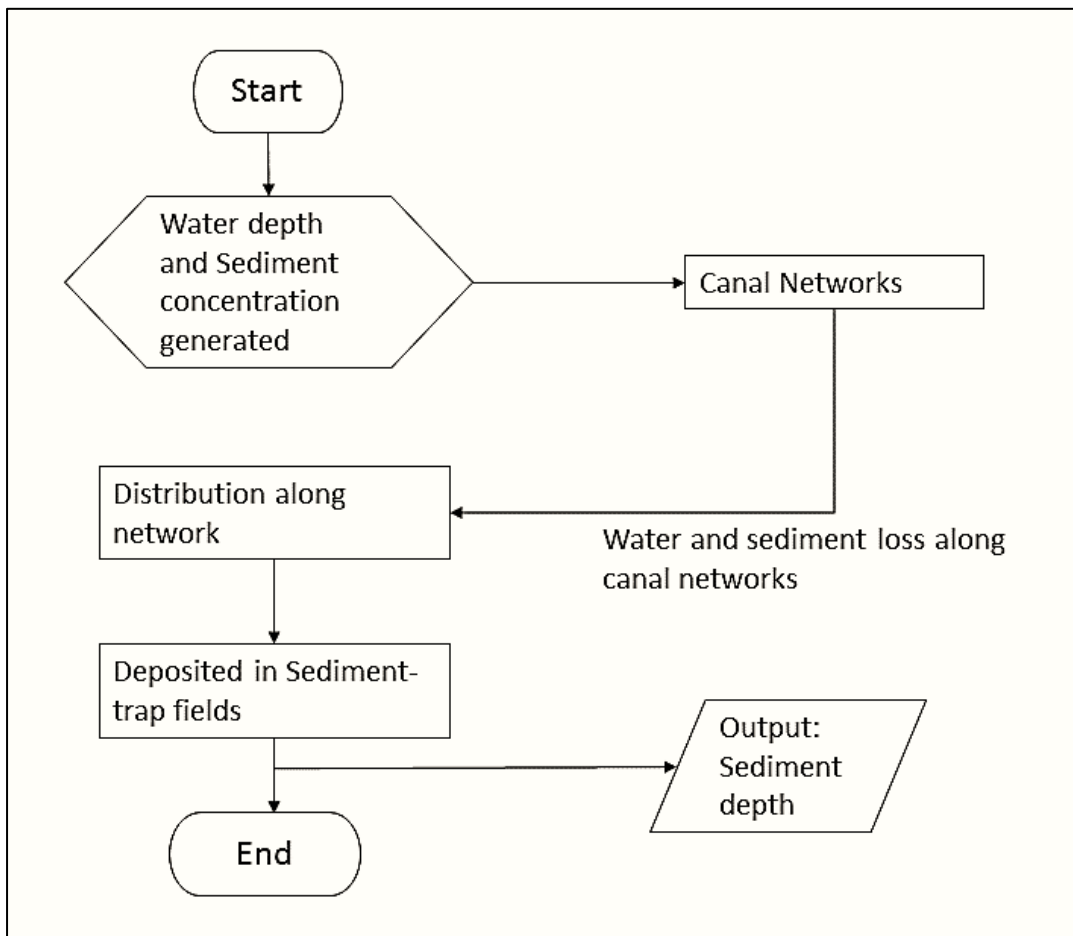
729 The sediment deposition and accumulation process comprises four stages i.e.
730 generation of water flows and sediments, water and sediment transport within the
731 irrigation canals, sediment discharge in the fields and sediment accumulation over
732 time. These processes occur within each year in the following order:

- 733 1. Water flows and sediment volumes are generated within the irrigation channels
734 and modelled on the principles of continuous uniform open channel flows. The
735 water flows and sediment volumes are distributed sequentially with the canalised
736 stream receiving water first and then being distributed into the irrigation canals
737 i.e. offtake canals and finally to the field offtake canals. In addition, the water
738 distributed is divided amongst the total number of canalised stream and irrigation
739 canals. In order to simulate water loss through seepage along the canalised
740 stream and irrigation canals, a parameter of water loss is incorporated such that
741 a certain proportion of the flows from the prior canal nodes are lost along the
742 canals.
- 743 2. Water and sediments are transported within the irrigation canals with the water
744 transporting suspended sediments. Similar to the water flows, some sediment

745 would be deposited along the water channels if the flows are not fast enough and
746 do not reach the fields. In order to simulate this phenomenon, sediment loss
747 along the canals was incorporated into the model.

- 748 3. Water and sediments are discharged into the fields from the irrigation canals.
- 749 4. Sediments that have been discharged accumulate over time in the fields; with
750 sediment accumulation a function of sediment discharge and bulk density and the
751 inverse of a soil consolidation factor for soil compaction over time.

752



753

754 Figure A. 1: Flow diagram of the ESTTraP model processes

755 The total flows, sediment discharge and sediment depth for all the fields are
756 collected at each time-step. The accumulation of sediments in the series of fields is
757 calculated on a daily time-step and the results analysed to determine the amount of
758 time required to accumulate the sediment depths that relate to the real world
759 observations and archaeological observations.

760

761 **A.3.2 ESTTraP Design concepts**

762 **Theoretical and Empirical background:** The water flows, and sediment transport
763 and deposition are modelled based on standard hydrological approaches including
764 streamflow hydrology and sedimentation dynamics. The estimation of water
765 discharge from the river channels and irrigation canals is based on the principles of
766 open channel continuous flows for trapezoidal channels with Manning's roughness
767 coefficient values within the range for natural streams with stone/pebble lined
768 channels and excavated channels with rubble sides and earth bottom slope (Chow,
769 1959) . The sediment discharge is estimated from a sediment rating curve, which is a
770 linear relationship of water discharge and total suspended sediments; while
771 sedimentation processes are based on the principles of sediment accumulation
772 (Robert, 2014, Wilkinson, et al., 2006, 7, Gordon, et al., 2004, van Rijn, 1984).

773

774 **Individual decision-making:** There is no individual decision-making.

775

776 **Learning:** There is no individual or collective learning included in the decision
777 model. The agents do not change the decision-making rules.

778

779 **Individual sensing:** There is no individual sensing.

780

781 **Individual prediction:** The model makes no predictions.

782

783 **Interactions:** The rate of water discharge has an effect on the discharge of
784 sediments, with a direct linear relationship between water and sediment discharge.

785

786 **Collectives:** The model contains no collectives.

787

788 **Heterogeneity:** There is no heterogeneity of decision-making by the agents.

789

790 **Stochasticity:** The amount of sediment discharged varies with changes in water
791 discharge which is in turn influenced by the water height within the river channels
792 and irrigation canals. In addition, the amount of water discharge decreases with
793 increase in distance from the main canalised stream.

794

795 **Observation:** The amount of sediments deposited within the fields is collected on a
796 daily time step. In addition, the water and sediment discharge from the canals is
797 observed. The amount of sediment that accumulates within each stone-bound field is
798 observed over time and the amount of water flows through the channels and canals
799 is also noted. The amount of time it takes for a field to accumulate sediments of up to
800 700 mm in depth is recorded. The data is compared between the varied
801 environmental scenarios of seasonal variability in water availability and erosive
802 processes i.e. as represented by changes in water depth in the canalised stream and
803 variations in suspended sediments, to determine the influence of these variations on
804 the rates of sediments transported, deposited and accumulated within the fields. In
805 addition the data is used for sensitivity analysis to assess the model's ability to
806 produce results highlighting the implications of these scenarios on the influence of
807 the water diversion infrastructure on field development and sediment accumulation
808 within the irrigation system.

809

810 **Emergence:** The key results emerging from the model are patterns of sediment
811 accumulation and field development over time, given the different environmental
812 scenarios of water availability.

813

814 **A.3.3 ESTTraP Details**

815 **Implementation Details**

816 The model is implemented in Windows 7 using the NETLOGO platform version 5.2.1
817 (Wilensky, 1999). The hydrological and sediment-transport model is implemented
818 through agents consisting of a network of nodes and directional links to represent the
819 irrigation channels that transport water and sediments to the fields. The nodes
820 contain information on the flow and sediment discharges along the system of
821 canalised stream and irrigation channels based on the agent characteristics. The
822 directed links that represent the irrigation channels distribute water and sediments
823 from the canalised stream into the fields via nodes set within each 6 x 6 m field. At
824 each time-step (representing the passage of one day) each node shares a
825 percentage of its value of sediments and water equally with its neighbours in the
826 network of nodes. The nodes also retain a percentage of the sediments and water
827 flows to represent sediment and diffusion loss incurred as these agents move along
828 the network. The transfer of sediments and water flows terminates at the fields,

829 where the nodes transfer these agents to the field patches as sediment discharge,
830 which is then converted to represent sediment accumulation.

831

832 **Initialisation**

833 Initial conditions for state variables in each grid cell (elevation in metres above sea
834 level, soil-depth in metres, and angle of slope) are derived from DEMs,
835 archaeological excavations and surveys of the study site. The initial values for the
836 water discharge and sediment discharge vary among simulations; however, some
837 initial values have been determined based on existing data. Initial values such as
838 water depth, used to determine cross sectional area of the channels and total
839 suspended sediments (TSS), were based on data from hydrological studies
840 conducted in 2015 along a 4 km² stretch of the Engaruka River. The irrigation
841 channel dimensions were based on archaeological measurements from studies
842 conducted by Stump in 2003 in the North Fields of the Engaruka field system
843 (Stump, 2006). The model has four sub-models that represent the water and
844 sediment discharge, irrigation canal networks and sediment accumulation. The
845 model parameters, their dimensions and default values are described in Table A.1
846 above.

847

848 **Input data**

849 The elevation data for the model was obtained using a digital elevation model, the
850 ASTER GDEM used is a product of METI and NASA (NASA_LP_DAAC, 2011). The
851 input data for the model parameters, variables and initial values are outlined in Table
852 A.1 above.

853

854 **Submodels**

855 The model runs on a daily time step with 365 steps per year, and with data collected
856 at each time step on the amount of sediment accumulated and changes in sediment
857 depth. The ESTTraP sub-models are described in Section 3 on material and
858 methods of the manuscript.

859

860 **Appendix B: Sensitivity and Uncertainty Analyses**

861 **B.1 Sensitivity and Uncertainty Analyses**

862 Global sensitivity analysis of the model was conducted using the NetLogo
863 BehaviorSpace and R 3.3.3 to explore the various model parameters in a systematic
864 way. This was in order to explore the model behaviour for varying parameters and
865 how they affect model outputs in order to see which parameters had the greatest
866 influence on model outputs. The outputs were then graphically visualised in R using
867 ggplot (Wickham, 2009) to assess the sensitivity of the model to variations in model
868 inputs. The three main parameters of TSS, water depth in channels and Manning’s
869 roughness coefficient (n) have a great influence on the output variables under
870 observation i.e. water and sediment discharge rates and the accumulation of
871 sediments within the fields. Global sensitivity analysis was conducted where the
872 selected input parameters for the model was run over all combinations of the main
873 parameters and iterated for 365 time steps to represent a year.

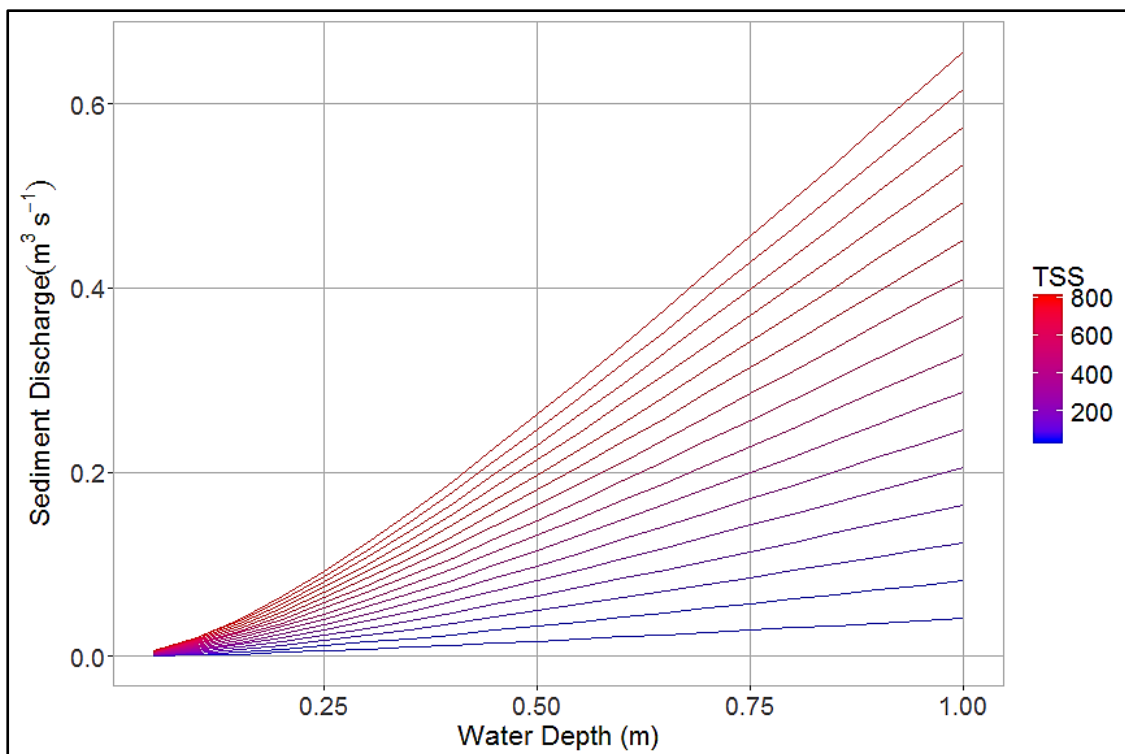
874 Table B.1: Model parameters used for global sensitivity analysis in BehaviorSpace

Parameter	Min value	Max value	Varied by
Water depth	0.05	1.0	0.05
TSS	50	800	50
Manning’s n	0.01	0.1	0.01

875
876 Exploratory global sensitivity analysis of the data shows that water and sediment
877 discharge varied with water depth while sediment discharge also varied with TSS. As
878 the water depth within the canalised streams and irrigation channels increased, the
879 amount of sediment being discharged into the stone-bound fields increased even as
880 the total suspended sediments were held constant (Figure B.1). This ties to existing
881 literature that estimates suspended sediment discharge through the linear
882 interpolation of estimated suspended sediment concentration and water discharge
883 (Gray and Simões, 2008, 1066). The increase in sediment discharge can be related
884 to the depth of the water column in the channels which allows for more water to flow
885 through at a given time and thus transport more sediment. This means that even in
886 instances where there is low sediment input from the surrounding catchment,
887 possibly due to vegetation cover, variations in the water depth from increased water
888 availability would influence the sediment discharge downstream. The water depth

889 and water discharge also affect sediment discharge particularly of fine sediments as
890 these fine particles can be transported at low water discharge rates (Steegeen, et al.,
891 2000, 31). This means that even in instances where water depth is low, sediment
892 discharge of fine sediments will still occur. Therefore where fine sediments such as
893 clay particles make up the majority of the total suspended sediment concentration,
894 low water depths and slower water discharge rates can effectively transport
895 sediments and the TSS volume becomes the predominant factor influencing
896 sediment discharge (Figure B.1).

897



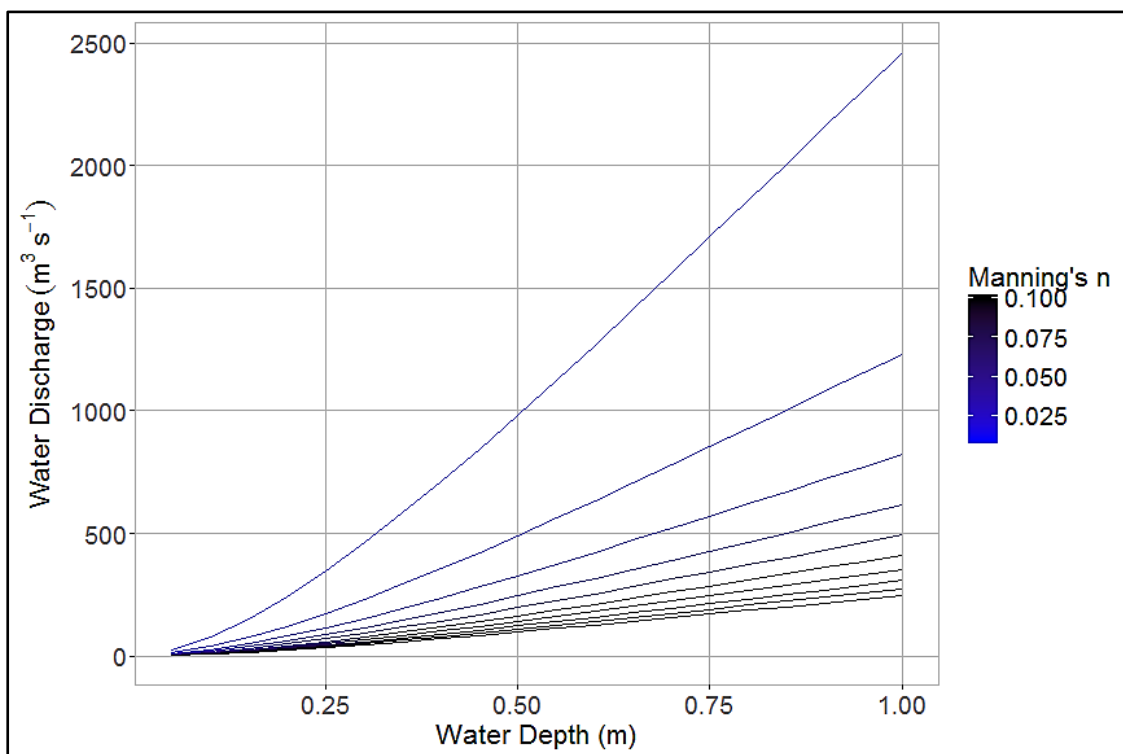
898

899 Figure B.1: Variations in mean annual sediment discharge ($\text{m}^3 \text{s}^{-1}$) with increasing
900 water depth and total suspended sediment (mg L^{-1}) with Manning's n of 0.03

901

902 The sediment discharge also increased with increased suspended sediment
903 volumes. Thus at a constant water depth increased TSS would result in increased
904 sediment discharge. This is relevant in representing increased incorporation of
905 sediments into the water channels during rain storm events and understanding the
906 changes in sediment discharge between different seasons. Studies by Nu-Fang
907 (2011) found that suspended sediment yield varied with the different seasons and
908 was highest when water availability was greatest. The variability in TSS would
909 therefore also affect the amount of sediment discharged and accumulated within the

910 field system. Since sediment discharge is a linear function of water and TSS,
 911 increase in the TSS values would therefore result in increase in the sediment
 912 discharged and therefore the accumulation rates in the fields. For the purposes of
 913 this model, a combination of variation in water depth and constant TSS would
 914 support representation of seasonal variations that would influence sediment
 915 accumulation as outlined below. Results of field studies conducted on water
 916 channels in the Engaruka found TSS values ranging from 50 to 800 mg/L, with the
 917 average TSS of 200 mg L⁻¹. The model therefore uses initial TSS values of 200 mg
 918 L⁻¹ and focuses on variability in water depth to simulate for the effects on water and
 919 sediment discharge.



920
 921 Figure B.2: Change in mean annual water discharge (m³ s⁻¹) with increasing water
 922 depth and changing Manning's roughness coefficient (n) values, with TSS of 200 mg
 923 L⁻¹

924
 925 Water discharge was also found to vary with water depth and varying Manning's
 926 roughness coefficients (Figure B.2). An increase in the Manning's n resulted in a
 927 decrease in the water discharge while an increase in water depth in the channels
 928 resulted in an increase in water discharge across all Manning's n values. Low
 929 Manning's n values are typical of the surfaces of artificial channels made with
 930 materials intended to reduce friction while natural channel surfaces tend to have

931 higher roughness coefficients (Chow, 1959). Based on data from Stump (2006) from
932 excavations conducted in Engaruka, the water channels modelled can be described
933 as excavated or dredged, straight earth channels with earth bottoms and stone-lined
934 channel sides. The calibration for these channels can therefore be adjusted to
935 approximate n of 0.030 based on interpretation of Chow's (1959) reference
936 Manning's n values.

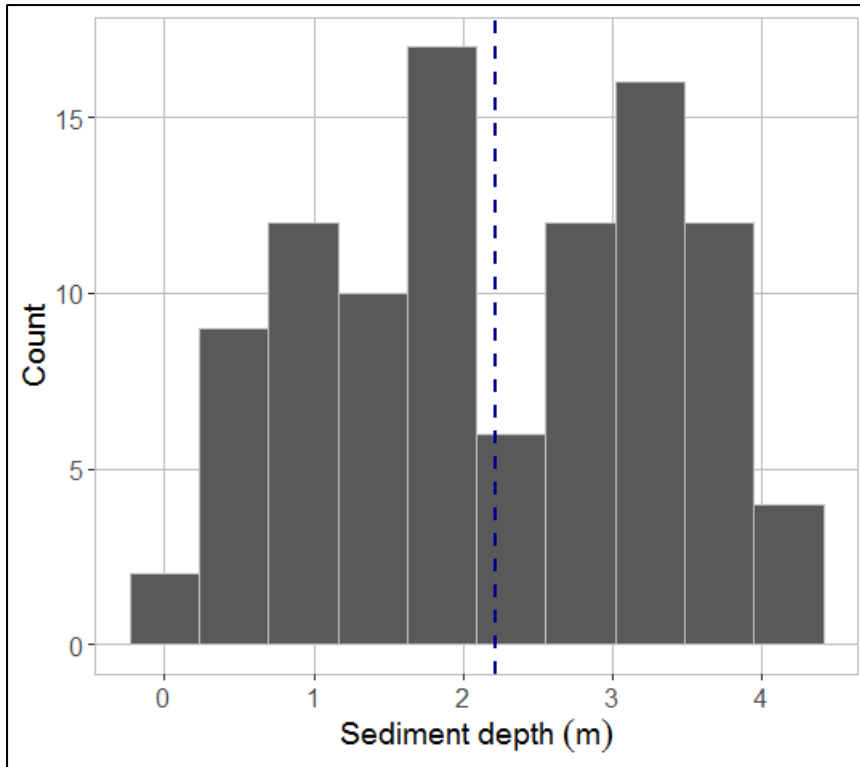
937 Increase in water depth resulted in increased water discharge (Figure B.2) and while
938 faster water discharge can seem useful in providing large supplies to fields, the high
939 water flows within the channels can result in damage to the channel walls by eroding
940 their surfaces. The preference would therefore be for lower water discharge at
941 channel water depths of less than 0.50 m. Calibration for other aspects of the cross-
942 sectional area of the channel i.e. bottom and top width and channel slope, were
943 based on the archaeological data from excavations conducted by Stump (2006). As
944 discussed above, sediment discharge can be interpolated from water discharge and
945 the model simulates the function as expected such that as water discharge increases
946 sediment discharge also increases.

947

948 Model Uncertainty analyses were conducted using NetLogo's BehaviorSpace where
949 the model scenario SIM-01 was run 100 times before stratified random sampling was
950 used to extract 100 random variables from the runs. These 100 runs were then
951 analysed using descriptive statistics in Excel to generate univariate statistics on the
952 variability and the central tendency of the sample group (Figure B.3).

953

954



955

956 Figure B.3: Histogram of 100 replicates displaying distribution of sediment depths
 957 for model outputs for SIM-01 scenario indicating the mean (blue dashed line). .

958

959 The summary statistics and histogram show that the data has a bimodal distribution
 960 with a mean of 2.21 m, standard deviation 1.14, sample variance of 1.30 and
 961 confidence level (95%) of 0.23. The peaks for the data fall within the range of the first
 962 quartile at 1.38m and the third quartile at 3.28m. This bimodality in the distribution of
 963 data can be due to selection of random variables from the data at different points in
 964 the time period as the model ran.

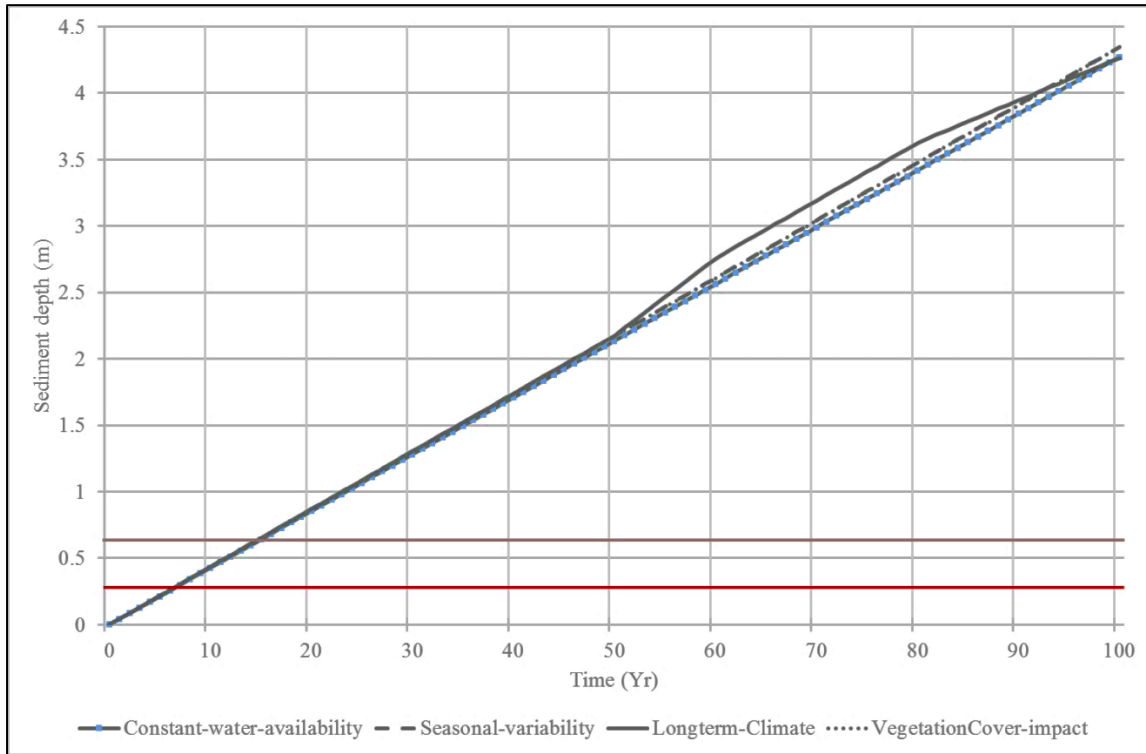
965

966 **B.2 Equivalence of Tested Scenarios**

967 The scenarios simulated utilised changes in water depth as proxies for the seasonal
 968 and long-term climate fluctuations that could affect water availability and thus water
 969 depth. The average daily water-depth for each scenario was determined where in
 970 SIM-01 average water-depth was 0.10 m per day, for SIM-02 the average daily water
 971 depth was 0.073 m, for SIM-03 the average daily water depth was 0.064 m, and for
 972 SIM-04 the average daily water depth was 0.093 m. This brings the question of
 973 whether the results of the scenarios simulated were due to the differences in
 974 average daily water depth or due to the trends in water depth over time. In order to

975 determine this the scenarios were also run with seasonal and long-term fluctuations
976 where water-depth would vary over different seasons but would still result in an
977 average daily water depth of 0.10 m overall in order to assess the equivalence of the
978 tested scenarios (Fig B.3).

979



980

981 Figure B.4: Mean annual cumulative sediment depth (metres) for constant water
982 availability (SIM-01), seasonal variability (SIM-02), long-term climate variability (SIM-
983 03), and vegetation cover impact (SIM-04) over a period of 100 years.

984

985 The results of the equivalence test showed that when the average daily water depth
986 was the same between the scenarios with different trends over time, the rates of
987 sediment accumulation closely matched. However it must be noted that in realistic
988 depictions of water availability, the seasonal and climate fluctuations mean that there
989 might be less water available in the water channels to transport water and sediments
990 to the fields thus these two variables are interlinked. The changes in water depth due
991 to differences in trends of water distribution as a result of seasonal and long-term
992 climate fluctuations would result in averaged daily water depths being lower than the
993 idealised rate, it would thus mean that it would be the combination of trends in water
994 distribution over time and the differences in water availability that would influence the
995 rate of sediment accumulation in the fields.

996

997 **Acknowledgements**

998 The Archaeology of Agricultural Resilience in Eastern Africa (AAREA) project is
999 funded by the European Research Council under the European Union's Seventh
1000 Framework Programme Starter Grant Scheme (FP/200702013/ERC); Grant
1001 Agreement No. ERC-StG-2012-337128-AAREA was awarded to D. Stump in
1002 February 2014. The research was also supported by funding awarded by the British
1003 Institute in East Africa to T.K. Kabora under the Thematic Research Grants
1004 2015/2016. The research in Tanzania was carried out under a research permit
1005 issued by the Tanzanian Commission for Science and Technology and an
1006 excavation license issued by the Antiquities Unit of the Ministry of Natural Resources
1007 and Tourism. The help and support provided by both these agencies is gratefully
1008 acknowledged. The authors would like to thank the anonymous peer reviewers for
1009 their comments and critiques that helped improve this paper, and in particular the
1010 authors would like to thank Iza Romanowska for taking the time to review the model
1011 code.

1012

1013 **References**

- 1014 Mekonnen, M., Keesstra, S.D., Stroosnijder, L., Baartman, J.E.M., Maroulis, J.,
1015 2015. Soil Conservation Through Sediment Trapping: A Review, *Land Degradation &*
1016 *Development* 26, 544-556.
- 1017 Beckers, B., Berking, J., Schütt, B., 2013. Ancient water harvesting methods in the
1018 drylands of the Mediterranean and Western Asia, *eTopoi. Journal for Ancient*
1019 *Studies*.
- 1020 Ferro-Vázquez, C., Lang, C., Kaal, J., Stump, D., 2017. When is a terrace not a
1021 terrace? The importance of understanding landscape evolution in studies of terraced
1022 agriculture, *Journal of Environmental Management* 202, 500-513.
- 1023 Hill, J., Woodland, W., 2003. Contrasting water management techniques in Tunisia:
1024 towards sustainable agricultural use, *The Geographical Journal* 169, 342-357.

- 1025 Giráldez, J.V., Ayuso, J.L., Garcia, A., López, J.G., Roldán, J., 1988. Water
1026 harvesting strategies in the semiarid climate of southeastern Spain, *Agricultural*
1027 *Water Management* 14, 253-263.
- 1028 Abedini, M., Md Said, M.A., Ahmad, F., 2012. Effectiveness of check dam to control
1029 soil erosion in a tropical catchment (The Ulu Kinta Basin), *CATENA* 97, 63-70.
- 1030 Ran, D.-C., Luo, Q.-H., Zhou, Z.-H., Wang, G.-Q., Zhang, X.-H., 2008. Sediment
1031 retention by check dams in the Hekouzhen-Longmen Section of the Yellow River,
1032 *International Journal of Sediment Research* 23, 159-166.
- 1033 Fisher, C., 2019. Archaeology for Sustainable Agriculture, *Journal of Archaeological*
1034 *Research*.
- 1035 Logan, A.L., Stump, D., Goldstein, S.T., Orijemie, E.A., Schoeman, M.H., 2019.
1036 Usable Pasts Forum: Critically Engaging Food Security, *Afr Archaeol Rev* 36, 419-
1037 438.
- 1038 Evenari, M., Shanan, L., Tadmor, N., 1982. *The Negev: the challenge of a desert*,
1039 Harvard University Press.
- 1040 Morrison, K.D., 2015. Archaeologies of flow: Water and the landscapes of Southern
1041 India past, present, and future, *Journal of Field Archaeology* 40, 560-580.
- 1042 Sheridan, M.J., 2002. An Irrigation Intake Is like a Uterus: Culture and Agriculture in
1043 Precolonial North Pare, Tanzania, *American Anthropologist* 104, 79-92.
- 1044 Stump, D., 2016. Digging for Indigenous Knowledge: 'Reverse Engineering' and
1045 Stratigraphic Sequencing as a Potential Archaeological Contribution to Sustainability
1046 Assessments, in: Isendahl, C., Stump, D. (Eds.), *The Oxford Handbook of Historical*
1047 *Ecology and Applied Archaeology*, Oxford University Press, Oxford Handbooks
1048 Online.
- 1049 Stump, D., 2006. The development and expansion of the field and irrigation systems
1050 at Engaruka, Tanzania, *AZANIA: Journal of the British Institute in Eastern Africa* 41,
1051 69-94.

- 1052 Lang, C., Stump, D., 2017. Geoarchaeological evidence for the construction,
1053 irrigation, cultivation, and resilience of 15th--18th century AD terraced landscape at
1054 Engaruka, Tanzania, *Quaternary Research*, 1-18.
- 1055 Ryner, M., Holmgren, K., Taylor, D., 2008. A record of vegetation dynamics and lake
1056 level changes from Lake Emakat, northern Tanzania, during the last c. 1200 years, *J*
1057 *Paleolimnol* 40, 583-601.
- 1058 Verschuren, D., Laird, K.R., Cumming, B.F., 2000. Rainfall and drought in equatorial
1059 east Africa during the past 1,100 years, *Nature* 403, 410-414.
- 1060 Ding, Z., Gong, W., Li, S., wu, Z., 2018. System Dynamics versus Agent-Based
1061 Modeling: A Review of Complexity Simulation in Construction Waste Management,
1062 *Sustainability* 10, 2484.
- 1063 Martin, R., Schlüter, M., 2015. Combining system dynamics and agent-based
1064 modeling to analyze social-ecological interactions—an example from modeling
1065 restoration of a shallow lake, *Frontiers in Environmental Science* 3.
- 1066 Siebers, P.O., Macal, C.M., Garnett, J., Buxton, D., Pidd, M., 2010. Discrete-event
1067 simulation is dead, long live agent-based simulation!, *J. Simul.* 4, 204-210.
- 1068 Bonabeau, E., 2002. Agent-based modeling: Methods and techniques for simulating
1069 human systems, *Proceedings of the National Academy of Sciences* 99, 7280-7287.
- 1070 Barton, M.C., 2016. From Narratives to Algorithms: Extending Archaeological
1071 Explanation beyond Archaeology, in: Isendahl, C., Stump, D. (Eds.), *The Oxford*
1072 *Handbook of Historical Ecology and Applied Archaeology*, Oxford University Press,
1073 Oxford Handbooks Online.
- 1074 Westerberg, L.-O., Holmgren, K., Börjeson, L., Håkansson, N.T., Laulumaa, V.,
1075 Ryner, M., Öberg, H., 2010. The development of the ancient irrigation system at
1076 Engaruka, northern Tanzania: physical and societal factors, *Geographical Journal*
1077 176, 304-318.
- 1078 Sutton, J.E.G., 1978. Engaruka and its Waters, *Azania: Archaeological Research in*
1079 *Africa* 13, 37-70.

1080 Sutton, J.E.G., 1998. Engaruka: An Irrigation Agricultural Community in Northern
1081 Tanzania Before the Maasai, *Azania: Journal of the British Institute in Eastern Africa*
1082 33, 1-37.

1083 Laulumaa, V., 2006. Estimation of the population of ancient Engaruka—a new
1084 approach, *Azania: Archaeological Research in Africa* 41, 95-102.

1085 Esri, 2011. National Geographic [basemap]. Scale 1:144,000. National Geographic
1086 World Map. 13 December 2011.
1087 <http://www.arcgis.com/home/item.html?id=b9b1b422198944fbbd5250b3241691b6>.
1088 (15 February 2017).

1089 Doolittle, W.E., 2015. Expedience, Impermanence, and Unplanned
1090 Obsolescence The Coming-About of Agricultural Features and Landscapes, in:
1091 Isendahl, C., Stump, D., Doolittle, W.E. (Eds.), *The Oxford Handbook of Historical*
1092 *Ecology and Applied Archaeology*, Oxford University Press.

1093 Howard, J.B., 1993. A paleohydraulic approach to examining agricultural
1094 intensification in Hohokam irrigation systems. In Scarborough, V.L. and B.L. Isaac
1095 (eds.) *Economic Aspects of Water Management in the Prehispanic New World.*,
1096 *Research in Economic Anthropology Supplement* 7, 263-324.

1097 Doolittle, W.E., 1984. Agricultural Change as an Incremental Process, *Annals of the*
1098 *Association of American Geographers* 74, 124-137.

1099 Wilensky, U., 1999. NetLogo. <http://ccl.northwestern.edu/netlogo/>. Center for
1100 Connected Learning and Computer-Based Modeling, Northwestern University,
1101 Evanston, IL.

1102 Müller, B., Bohn, F., Dreßler, G., Groeneveld, J., Klassert, C., Martin, R., Schlüter,
1103 M., Schulze, J., Weise, H., Schwarz, N., 2013. Describing human decisions in agent-
1104 based models – ODD + D, an extension of the ODD protocol, *Environmental*
1105 *Modelling & Software* 48, 37-48.

1106 Grimm, V., Berger, U., Bastiansen, F., Eliassen, S., Ginot, V., Giske, J., Goss-
1107 Custard, J., Grand, T., Heinz, S.K., Huse, G., Huth, A., Jepsen, J.U., Jørgensen, C.,
1108 Mooij, W.M., Müller, B., Pe'er, G., Piou, C., Railsback, S.F., Robbins, A.M., Robbins,

1109 M.M., Rossmannith, E., Rüger, N., Strand, E., Souissi, S., Stillman, R.A., Vabø, R.,
1110 Visser, U., DeAngelis, D.L., 2006. A standard protocol for describing individual-
1111 based and agent-based models, *Ecol. Model.* 198, 115-126.

1112 NASA_LP_DAAC, 2011. ASTER Global Digital Elevation Model (GDEM) 1 arc
1113 second. Version 2. 03°S, 35°E. , NASA EOSDIS Land Processes Distributed Active
1114 Archive Center (LP DAAC), USGS Earth Resources Observation and Science
1115 (EROS) Center, Sioux Falls, South Dakota. [DOI:
1116 <http://dx.doi.org/10.5067/ASTER/ASTGTM.002>]

1117 Robert, A., 2014. *River processes: an introduction to fluvial dynamics*, Routledge.

1118 Van Rijn, L.C., 1993. *Principles of sediment transport in rivers, estuaries and coastal*
1119 *seas*, Aqua publications Amsterdam.

1120 van Rijn, L.C., 2013. *Sedimentation of Sand and Mud in Reservoirs in Rivers*.

1121 Wilkinson, S.N., Prosser, I.P., Hughes, A.O., 2006. Predicting the distribution of bed
1122 material accumulation using river network sediment budgets, *Water Resources*
1123 *Research* 42, n/a-n/a.

1124 McKenzie, N., Coughlan, K., Cresswell, H., 2002. *Soil physical measurement and*
1125 *interpretation for land evaluation*, Csiro Publishing.

1126 FAO, 2006. *Guidelines for Soil Description.*, 4 ed., Food and Agriculture
1127 Organization of the United Nations, Rome.

1128 Harris, I., Jones, P.D., Osborn, T.J., Lister, D.H., 2014. Updated high-resolution grids
1129 of monthly climatic observations – the CRU TS3.10 Dataset, *International Journal of*
1130 *Climatology* 34, 623-642.

1131 Thiele, J.C., Kurth, W., Grimm, V., 2014. Facilitating Parameter Estimation and
1132 Sensitivity Analysis of Agent-Based Models: A Cookbook Using NetLogo and 'R',
1133 *Journal of Artificial Societies and Social Simulation* 17, 11.

1134 Saltelli, A., Ratto, M., Andres, T., Campolongo, F., Cariboni, J., Gatelli, D., Saisana,
1135 M., Tarantola, S., 2008. *Global sensitivity analysis: the primer*, John Wiley & Sons.

1136 Seidel, M., Hlawitschka, M., 2015. An R-Based Function for Modeling of End
1137 Member Compositions, *Mathematical Geosciences* 47, 995-1007.

1138 Jones, P., Harris, I., 2008. Climatic Research Unit (CRU) time-series datasets of
1139 variations in climate with variations in other phenomena, NCAS British Atmospheric
1140 Data Centre.

1141 Marchant, R., Richer, S., Boles, O., Capitani, C., Courtney-Mustaphi, C.J., Lane, P.,
1142 Prendergast, M.E., Stump, D., De Cort, G., Kaplan, J.O., Phelps, L., Kay, A., Olago,
1143 D., Petek, N., Platts, P.J., Punwong, P., Widgren, M., Wynne-Jones, S., Ferro-
1144 Vázquez, C., Benard, J., Boivin, N., Crowther, A., Cuní-Sanchez, A., Deere, N.J.,
1145 Ekblom, A., Farmer, J., Finch, J., Fuller, D., Gaillard-Lemdahl, M.-J., Gillson, L.,
1146 Githumbi, E., Kabora, T., Kariuki, R., Kinyanjui, R., Kyazike, E., Lang, C., Lejju, J.,
1147 Morrison, K.D., Muiruri, V., Mumbi, C., Muthoni, R., Muzuka, A., Ndiema, E., Kabonyi
1148 Nzabandora, C., Onjala, I., Schrijver, A.P., Rucina, S., Shoemaker, A., Thornton-
1149 Barnett, S., van der Plas, G., Watson, E.E., Williamson, D., Wright, D., 2018. Drivers
1150 and trajectories of land cover change in East Africa: Human and environmental
1151 interactions from 6000 years ago to present, *Earth-Science Reviews* 178, 322-378.

1152 Barker, P., Gasse, F., 2003. New evidence for a reduced water balance in East
1153 Africa during the Last Glacial Maximum: implication for model-data comparison,
1154 *Quaternary Science Reviews* 22, 823-837.

1155 Lesschen, J.P., Schoorl, J.M., Cammeraat, L., 2009. Modelling runoff and erosion for
1156 a semi-arid catchment using a multi-scale approach based on hydrological
1157 connectivity, *Geomorphology* 109, 174-183.

1158 Wainwright, J., 2008. Can modelling enable us to understand the rôle of humans in
1159 landscape evolution?, *Geoforum* 39, 659-674.

1160 Linard, J.I., Wolock, D.M., Webb, R.M., Wieczorek, M.E., 2009. Identifying hydrologic
1161 processes in agricultural watersheds using precipitation-runoff models, US
1162 Geological Survey.

1163 Montgomery, D.R., Buffington, J.M., 1998. Channel processes, classification, and
1164 response, in: Naiman, R.J., Bilby, R.E. (Eds.), *River Ecology and Management:
1165 Lessons from the Pacific Coastal Ecoregion*, Springer, New York, pp. 13 - 42.

1166 Miedema, S., 2010. Constructing the Shields curve, a new theoretical approach and
1167 its applications, WODCON XIX, Beijing China.

1168 Sundborg, Å., 1956. The River Klarälven: A Study of Fluvial Processes, *Geografiska
1169 Annaler* 38, 125-237.

1170 Chow, T.V., 1959. *Open-channel hydraulics*, McGraw-Hill.

1171 Gordon, N.D., McMahon, T.A., Finlayson, B.L., 2004. *Stream hydrology: an
1172 introduction for ecologists*, John Wiley and Sons.

1173 van Rijn, L.C., 1984. Sediment Transport 2: Suspended load transport, *J. Hydraul.
1174 Eng.-ASCE* 110, 1613-1641.

1175 Wickham, H., 2009. *ggplot2: Elegant Graphics for Data Analysis*, Springer-Verlag
1176 New York.

1177 Gray, J.R., Simões, F.J., 2008. Estimating sediment discharge, *Sedimentation
1178 Engineering: Processes, Measurements, Modeling, and Practice*, pp. 1067-1088.

1179 Steegen, A., Govers, G., Nachtergaele, J., Takken, I., Beuselinck, L., Poesen, J.,
1180 2000. Sediment export by water from an agricultural catchment in the Loam Belt of
1181 central Belgium, *Geomorphology* 33, 25-36.

1182 Nu-Fang, F., Zhi-Hua, S., Lu, L., Cheng, J., 2011. Rainfall, runoff, and suspended
1183 sediment delivery relationships in a small agricultural watershed of the Three Gorges
1184 area, China, *Geomorphology* 135, 158-166.

1185